MODELING PREDICTIVE SUITABILITY TO ESTIMATE THE POTENTIAL OF WIND AND SOLAR ENERGY TO POWER WATER DESALINATION UNITS IN GÜZELYURT REGION, NORTHERN CYPRUS

**A THESIS SUBMITTED TO THE GRADUATE SCHOOL OF APPLIED SCIENCES
OF
NEAR EAST UNIVERSITY**

**By
RIFAT GÖKÇEKUŞ**

**In Partial Fulfillment of the Requirements for the Degree of Master
in
CIVIL Engineering**

NICOSIA, 2021

RIFAT GÖKÇEKUŞ
MODELING PREDICTIVE SUITABILITY TO ESTIMATE THE POTENTIAL OF WIND AND SOLAR ENERGY TO POWER WATER DESALINATION UNITS IN GÜZELYURT REGION, NORTHERN CYPRUS
NEU
2021

MODELING PREDICTIVE SUITABILITY TO ESTIMATE THE POTENTIAL OF WIND AND SOLAR ENERGY TO POWER WATER DESALINATION UNITS IN GÜZELYURT REGION, NORTHERN CYPRUS

A THESIS SUBMITTED TO THE GRADUATE

SCHOOL OF APPLIED SCIENCES

OF

NEAR EAST UNIVERSITY

By

RIFAT GÖKÇEKUŞ

In Partial Fulfillment of the Requirements for the Degree of Master of Science in Civil Engineering

NICOSIA, 2021

Rifat Gökçekuş: MODELING PREDICTIVE SUITABILITY TO ESTIMATE THE POTENTIAL OF WIND AND SOLAR ENERGY TO POWER WATER DESALINATION UNITS IN GÜZELYURT REGION, NORTHERN CYPRUS

Approval of Director of Graduate School of Applied Sciences

Prof. Dr. K. Hüsnü Can Başer

We certify this thesis is satisfactory for the award of the degree of Master of Science in Mechanical Engineering

Examining Committee in Charge:

Prof. Dr. Hüseyin GÖKÇEKUŞ	Committee Chairman, Department of Civil Engineering, NEU
Assoc. Prof. Dr. Hüseyin ÇAMUR	Department of Mechanical Engineering, NEU
Assoc. Prof. Dr. Fidan Aslanova	Department of Civil Engineering, NEU
Assist. Prof. Dr. Anoosheh Iravanian	Supervisor, Department of Civil Engineering, NEU
Assoc. Prof. Dr. Youssef Kassem	Co-supervisor, Department of Mechanical Engineering, NEU

I hereby declare that, all the information in this document has been obtained and presented in accordance with academic rules and ethical conduct. I also declare that, as required by these rules and conduct, I have fully cited and referenced all material and results that are not original to this work.

Name, Last Name: Rifat Gökçekuş

Signature: 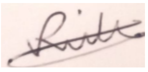

Date: 20/09/2021

ACKNOWLEDGEMENTS

I would like to articulate our deep gratitude to our project guide Assist. Prof. Dr. Anoosheh Iravanian and Assoc. Prof. Dr. Youssef Kassem have always been sources of motivation and firm support for carrying out the project. I express our gratitude to Prof. Dr. Hüseyin Gökçekuş for his invaluable suggestions and encouragement all through the thesis work.

I would also like to convey our sincerest gratitude and indebtedness to all other faculty members and staff of Department of Civil Engineering Department, who bestowed their great effort and guidance.

I owe a special thanks to our friends for their valuable suggestions and help during the course of the project.

Further, I would like to express our feeling towards my parents who directly or indirectly encouraged and motivated us during this dissertation

To my parents….

ABSTRACT

In Northern Cyprus, groundwater is overexploited causing the water table to decline below the sea level and has high levels of salinity and classified as “hard to very hard” and “slightly alkaline to alkaline” based on the reviewed previous scientific studies. Presently, water, which is used drinking and domestic used, comes mainly from the water pipeline project of Turkey-North Cyprus via a pipeline under the Mediterranean Sea to Northern Cyprus. However, the island experienced a water shortage in summer 2020 due to serious damage to the water pipeline. Therefore, a water desalination unit that is powered by renewable energy is a good solution for desalting groundwater for domestic purposes on the island. In this study, the Güzelyurt region (agriculture region) was selected since it faced great challenges due to chemical contamination and intrusion of seawater in the groundwater sources. The objective of this study is to investigate the potential of wind and solar energy in the selected region based on 33-year meteorological data (wind speed, global solar radiation, air temperature, and sunshine duration). The results demonstrate that Burr (4P), Wakeby and Generalize Extreme Value are considered as an effective distribution among 37 distribution functions to analyze the characteristics of wind speed in the region. Also, the results showed that the region has huge solar energy potential compared to wind energy potential. Consequently, the present paper has investigated the feasibility of small-scale grid-connected PV systems with various sun-tracking systems as power sources to satisfying the farms' electric and water needs. The results show that the proposed system with Two-axis sun-tracking system can provide effective solutions for energy poverty in regions with very positive socio-economic and environmental impacts. Also, the small-scale grid-connected PV system will provide the farms' electric and water needs at energy production costs lower than the electricity price grid-connected consumers pay. Finally, this study is tried to increase awareness about utilizing PV sun-tracking systems and the feasibility of small-scale grid-connected rooftop PV systems in the selected regions.

Keywords: Northern Cyprus; grid-connected; wind potential; solar potential; techno-economic; sun-tracking system

ÖZET

Kuzey Kıbrıs Türk Cumhuriyeti'nde yeraltı sularının aşırı kullanımı sebebi ile su tablası deniz seviyesinin altına düşmüş ve aşırı derecede tuzlanmaya neden olmuştur. Önceki bilimsel çalışmalar ışığında tuzlanmanın etkisiyle yeraltı suları 'sert-çok sert' ve 'hafif alkali- alkali' olarak sınıflandırılmıştır. Hâlihazırda içme suyu ve kullanma suyu, TC-KKTC Deniz Altı Boru Hattı Projesi kapsamında Geçitköy Barajı'nda toplanmaktadır. Ancak, boru hattının ciddi şekilde hasar görmesi nedeniyle 2020 yılı yaz ayında adada su sıkıntısı yaşanmıştır. Bu nedenle, yenilenebilir enerji ile çalışan suyu tuzdan arındırma ünitesinin, evsel amaçlarla yeraltı suyu tuzunun giderilmesi için iyi bir çözüm olacağı düşünülmüştür. Bu araştırmada, kimyasal kirlenme ve deniz suyunun yeraltı suyu kaynaklarına karışması nedeniyle büyük zorluklarla karşı karşıya kalan Güzelyurt bölgesi (tarım bölgesi) seçilmiştir. Bu araştırmanın amacı, 33 yıllık meteorolojik verilere (rüzgâr hızı, küresel Güneş radyasyonu, hava sıcaklığı ve güneşlenme süresi) dayanarak seçilen bölgedeki rüzgâr ve güneş enerjisi potansiyelini incelemektir. Sonuçlar; bölgedeki rüzgâr hızının özelliklerini analiz etmek için Burr (4P), Wakeby ve Generalize Extreme Value'nin 37 dağıtım fonksiyonu arasında etkili bir dağılım gösterdiğini ortaya koymuştur. Ayrıca sonuçlar, bölgenin rüzgâr enerjisi potansiyeline kıyasla çok büyük Güneş enerjisi potansiyeline sahip olduğunu göstermiştir. Sonuç olarak bu araştırmada, Tarım arazilerinin elektrik ve su ihtiyacını karşılamak için güç kaynağı olarak çeşitli güneş izleme sistemlerine sahip küçük ölçekli şebeke bağlantılı PV sistemleri incelenmiştir. Sonuçlar, iki eksenli Güneş takip sistemi ile önerilen sistemin, sosyo-ekonomik ve çevresel etkileri çok olumlu olan bölgelerde enerji yoksunluğuna etkin çözümler sağlayabileceğini göstermiştir. Ayrıca, küçük ölçekli şebekeye bağlı PV sistemi, tarım arazilerinin elektrik ve su ihtiyacını, şebekeye bağlı tüketicilerin ödediği elektrik fiyatından daha düşük enerji üretim maliyetiyle sağlayacaktır. Son olarak, araştırma ile, seçilen bölgelerde PV Güneş izleme sistemlerinin kullanımını ve küçük ölçekli şebekeye bağlı çatı PV sistemlerinin fizibilitesi konusunda farkındalığı artırmaya çalışılmıştır.

Anahtar Kelimeler: Kuzey Kıbrıs; şebeke bağlantılı; rüzgâr potansiyeli; güneş potansiyeli; ekonomik; güneş takip sistemi.

TABLE OF CONTENTS

LIST OF TABLES

LIST OF FIGURES

CHAPTER 1
INTRODUCTION

1.1 Background

Water scarcity is one of the essential issues facing the world due to growth of population and the increasing pressure on the water resources consumption. Two-thirds of the world's population may face water scarcity due to over extraction of groundwater reserves or pollution of existing surface water resources (Clemens et al. 2020; Rezaei et al., 2019; Jia et al. 2018). Moreover, climate change has led to reduce the availability of groundwater resources, which is one-third of all freshwater withdrawals used for domestic, agricultural and industrial purposes (Döll et al. 2012).

In recent years, the trend of water shortage has been increased due to the growth of population, decreased rainfall, and water management issues (Aparicio et al. 2017). According to the World Water Assessment Programme (2015), the water shortage is expected to affect more than 40% of the world's inhabitants. Moreover, drought and salinization problems are serious problems for most of the Mediterranean countries including Cyprus. Therefore, desalination systems can be an alternative solution for solving the water shortage for drinking or irrigation purposes (Fritzmann et al. 2007; Mansouri et al. 2020). Desalination is the process of the removal the salts from the feedwater, typically containing a high concentration of salts to produce freshwater containing a low concentration of salts (Khan et al. 2018; Mostafaeipour et al. 2019). In general, desalination processes is classified based on two main desalination technologies; (1) desalination based thermal vapor generation and (2) desalination based thermal vapor compression (Elmaadawy et al. 2020; Li et al. 2018).

Reverse Osmosis (RO) membrane technology is widespread technology. RO is routinely used to remove salt from groundwater in small/medium/large scale decentralized plants. Several factors could be related to this shift such as lowers energy consumption (Al-Karaghouli and Kazmerski 2013; Greenlee et al. 2009), the ability to remove 95%-99% of TDS along with nearly 100% of heavy metals, organic matter, viruses, and bacteria (Hoslett et al. 2018; Ezugbe and Rathilal 2020), easy to operate/maintain, and have lower environmental impacts (Ahmad and Schmid 2000; Muñoz and Fernández-Alba 2008). RO is carried out by motor-pumps and semi-permeable membranes (Khiari et al. 2019). In the literature, Cyprus has two large seawater reverse osmosis desalination namely, Dhekelia and Larnaca with a plant capacity of 60,000 m3/d and 40,000m3/d, respectively (Kim et al. 2019; Farhat et al. 2020).

In general, the processes of desalination require significant quantities of energy. Thus, renewable energy sources can be considered a viable alternative and eco-friendly energy source to power the desalination plants, to reduce the dependency on fossil fuel for water desalination and minimize the cost and risk of water distribution. Numerous scientific studies concluded that the integration of desalination and renewable energy technologies for freshwater production is a good solution for solving the shortage of water and desalting the groundwater for drinking/irrigation purposes (Mahmoudi et al. 2009; Akhatov et al. 2011; Triki et al. 2013; Wright and Winter 2014; Gökçek and Gökçek 2016; Gökçek, 2018; Wu et al. 2018; Vakili-Nezhaad et al. 2019; Fodhil et al. 2019; Monjezi et al. 2020). For example, Wright and Winter (2014) concluded that PV-powered electrodialysis would meet the water demands of rural Indian villages due to its viability and reduce the energy required. Peng et al. (2018) found that hybrid renewable energy systems including photovoltaic panels, wind turbines, battery banks, and reverse osmosis desalination increased the reliability of the system for increasing the availability of freshwater. Fodhil et al. (2019) found that a hybrid grid-connected PV system has the potential to supply significant power for seawater desalination stations. Besides, Monjezi et al. (2020) found that coupling solar photovoltaic thermal cells to RO desalination could be led to a reduction of 0.12 kWh/m3 in the specific electricity consumption rate of RO desalination.

1.2 Scope of the Study

According to Kassem et al. (2020), the solar power system could be utilized as power sources to reduce high-energy consumption and CO2 emissions in Northern Cyprus compared to the wind system (Alayat et al. 2018; Kassem et al. 2018). Furthermore, the previous scientific studies (Gökçekuş and Doyuran 1997; Gökçekuş et al. 2002; Gökçekuş and Nourani 2018; Arslan and Akün 2019) concluded that Güzelyurt agriculture faces great challenges due to chemical contamination and intrusion of seawater in the groundwater sources.

Moreover, in the literature, a lot of the scientific studies carried out on utilizing the renewable energies in RO plants in off-grid mode, however, few studies have considered the grid-connected mode. Fodhil et al. (2019) utilized the grid-connected PV system as a power source for the 2500m3/d seawater RO desalination plant. Moser et al. (2013) compared different renewable energy options to power RO and multiple-effect distillation plants by using two methods; (i) suggested grid compensation and (ii) suggested the addition of an equivalent firm power supply capacity to cover the energy shortage. Ko et al. (2013) developed a new approach of a grid-connected seawater reverse osmosis based on energy cost reduction.

Therefore, the present study focuses on the economic and financial assessment of utilizing wind energy and solar energy as a power source for the saline water desalination in the agricultural region (Güzelyurt) and generating electricity for the household. To achieve this, the solar and wind energy characteristics in the selected regions are analyzed based on a 33-year database (1985 -2017). For wind energy potential, 37 distribution functions are utilized to identify the suitable probability functions for estimating the wind energy potential in the selected region. Goodness-of-fit tests including Kolmogorov–Smirnov (K-S) test, Anderson–Darling (A-D) test, and Chi-squared (C-s) test are used to select the best-fit probability distribution model. For solar energy potential, the solar radiation data, air temperature and sunshine duration, which obtained from the Meteorological department, are analyzed.

Generally, utilizing wind and solar systems can help to reduce the pressure on freshwater and conventional energy consumption as well as, to reduce CO_2 emissions associated with fossil fuel. In this regard, three small RO desalination plant is designed to meet the water needs for the household and farm. The power requirement of the RO desalination plants is calculated to develop a grid-connected solar or wind system. The structure of the proposed system in the present study is illustrated in Figure 1.1.

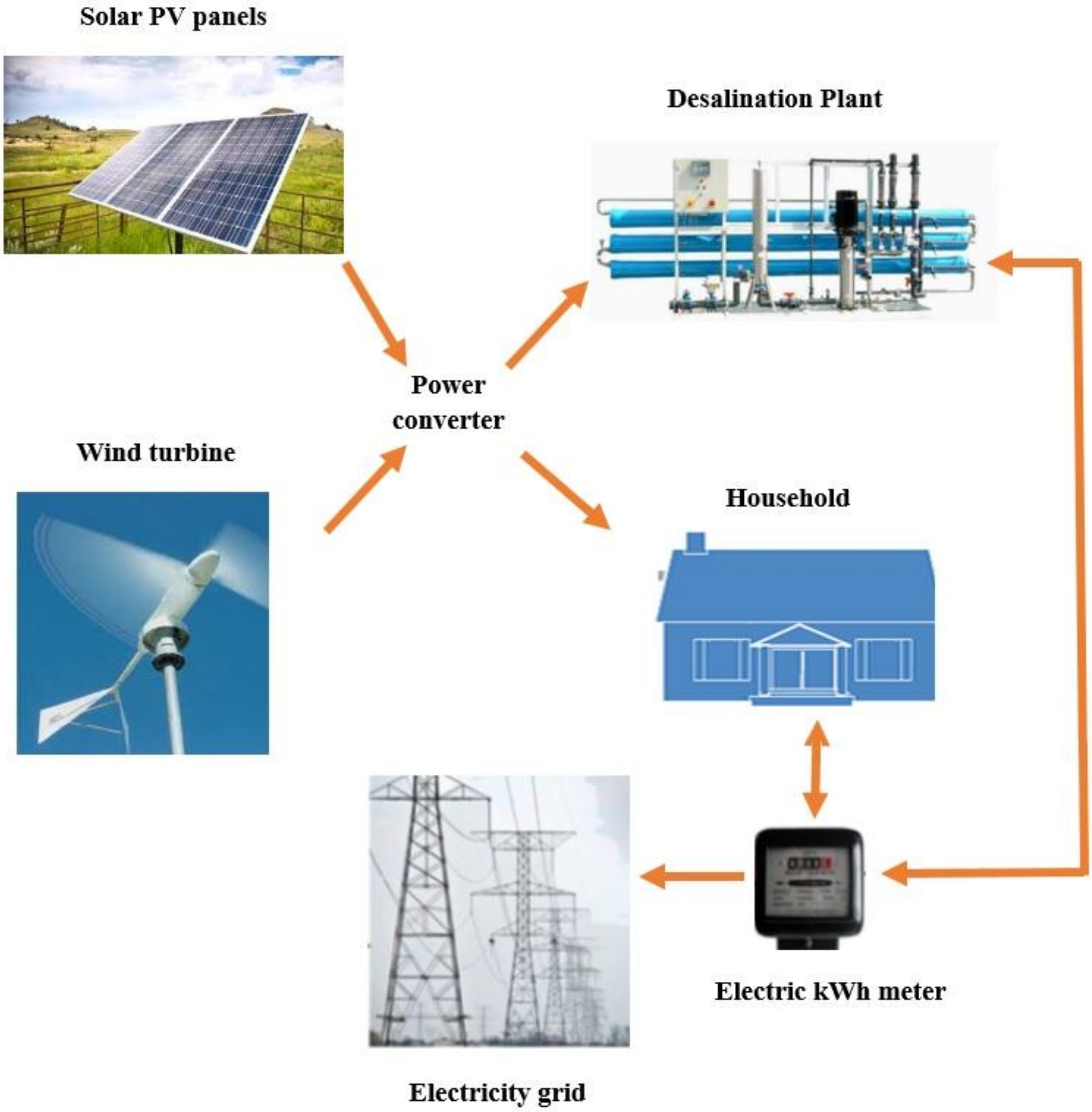

Figure 1.1: Schematic of a typical grid-connected wind/solar power system for household and desalination plant

1.2 Research Outline

The importance of renewable energy to the world is discussed in this chapter. The water resources and agriculture potential in Northern Cyprus are presented in Chapter 2. Moreover, the methodology that used to investigate the potential of solar and wind energy is explained in Chapter 3. In Chapter 4 all test results are displayed for the proposed system. On the end of the dissertation, the conclusions are presented in Chapter 5.

CHAPTER 2
WATER RESOURCE AND AGRICULTURE POTENTIAL

2.1 Water resources in Northern Cyprus

The water resources in Cyprus are classified into groundwater resources (75.5%), semi-perennial low-discharge springs (0.3%), several surface water reservoirs (20.4%), and few small-scale treatment plants (3.8%) (Elkiran et al. 2020). Figure 2.1 shows the main river basins in Northern Cyprus. Also, Figure 2.2 shows the streams in Northern Cyprus.

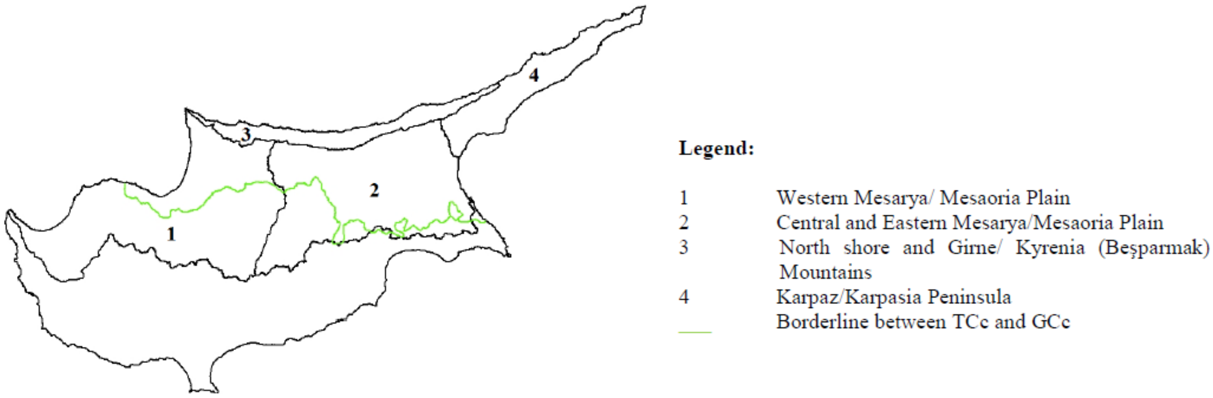

Figure 2.1: Main river basins of the northern part of Cyprus (Türker and Hansen, 2012)

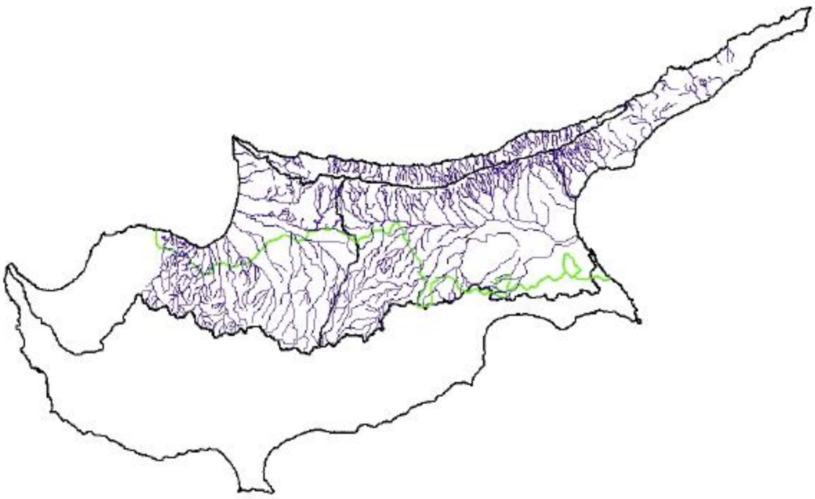

Figure 2.2: Streams in the northern part of Cyprus (Türker and Hansen, 2012)

Furthermore, the estimated annual volume provided for irrigation and groundwater recharge is approximately 8.4 mill m3, which means about 33% of the operational storage capacity is used for irrigation purposes (Kassem et al. 2020). Besides, based on theoretical estimation for surface water stored volume for groundwater purposes, it is found that around 14% of the operational storage capacity is used for groundwater recharge (Kassem et al. 2020). Also, it is estimated that about 30-40% of water stored is lost due to evaporation (Kassem et al. 2020). Table 2.1 shows some selected dams in Northern Cyprus with their capacity and year of construction.

Table 2.1: Constructed dams in Northern Cyprus (Agboola and Egelioglu, 2012)

District	Dams	Year of construction	Capacity (10^3) [m^3]	Irrigation area [ha]
Gazimağusa	Gönendere	1987	940	150
	Geçitkale	1989	1360	240
	Mersinlik	1989	1140	170
	Tatlisu	1989	156	50
	Ergazi	1989	400	84
Güzelyurt	Akdeniz	1988	1470	-
	Gemikonağı	1988	4120	-
Girne	Geçitköy	1989	1800	161
	Zeytinlik	1989	50	-
	Karsiyaka	1989	25	-
	Arapköy 1	1990	440	40
	Arapköy 2	1990	600	65
	Beşparmak	1992	775	67
	Dağyolu	1994	392	82
Lefkoşa	Değirmenlik	1990	297	30
	Hamitköy	1992	529	95
	Serdarli	1992	391	56
	Lefkoşa	1994	517	40

The Güzelyurt groundwater basin is located within the western part of Northern Cyprus (Figure 2.3). Since 1957, increasing rates of pump-age have caused a progressive decline in the groundwater levels, locally reaching 45-50 m below mean sea level (Gökçekuş and Nourani 2018; Gökçekus and Doyuran 1995; Arslan and Akün 2019). Limited natural recharge and excessive withdrawals from approximately 250 active municipal and irrigation wells have not only produced a considerable reduction in the aquifer storage but also degradation of groundwater quality due to saltwater intrusion and bedrock contamination (Gökçekuş and Nourani 2018). The aquifer provides the main source of potable water. The total basin area of the Aquifer is around 460 km2 of which 1/3 of this area is under the control of the Greek Cypriot Community and 2/3 is under the control of Turkish Cypriot Community Authorities (Sofroniou and Bishop 2014). Most of the aquifers in the northern part of Cyprus are unconfined (phreatic) made up of the river or coastal alluvial deposits, mainly silts, sands, and gravels (Ergil 2000). The main aquifers in the north part of Cyprus are Girne mountain aquifer, which is located in Beşparmak Mountains close to the north coast, Güzelyurt aquifer, located in western Mesarya, and Gazimağusa aquifer, located in Southeastern Mesarya.

The aquifers are mainly being recharged by rainfall and river flows (in a very limited period of the year) and are more or less all showing trends of depletion due to reduced recharging, frequent droughts, and increased abstraction mainly by farmers in their effort to increase their production level.

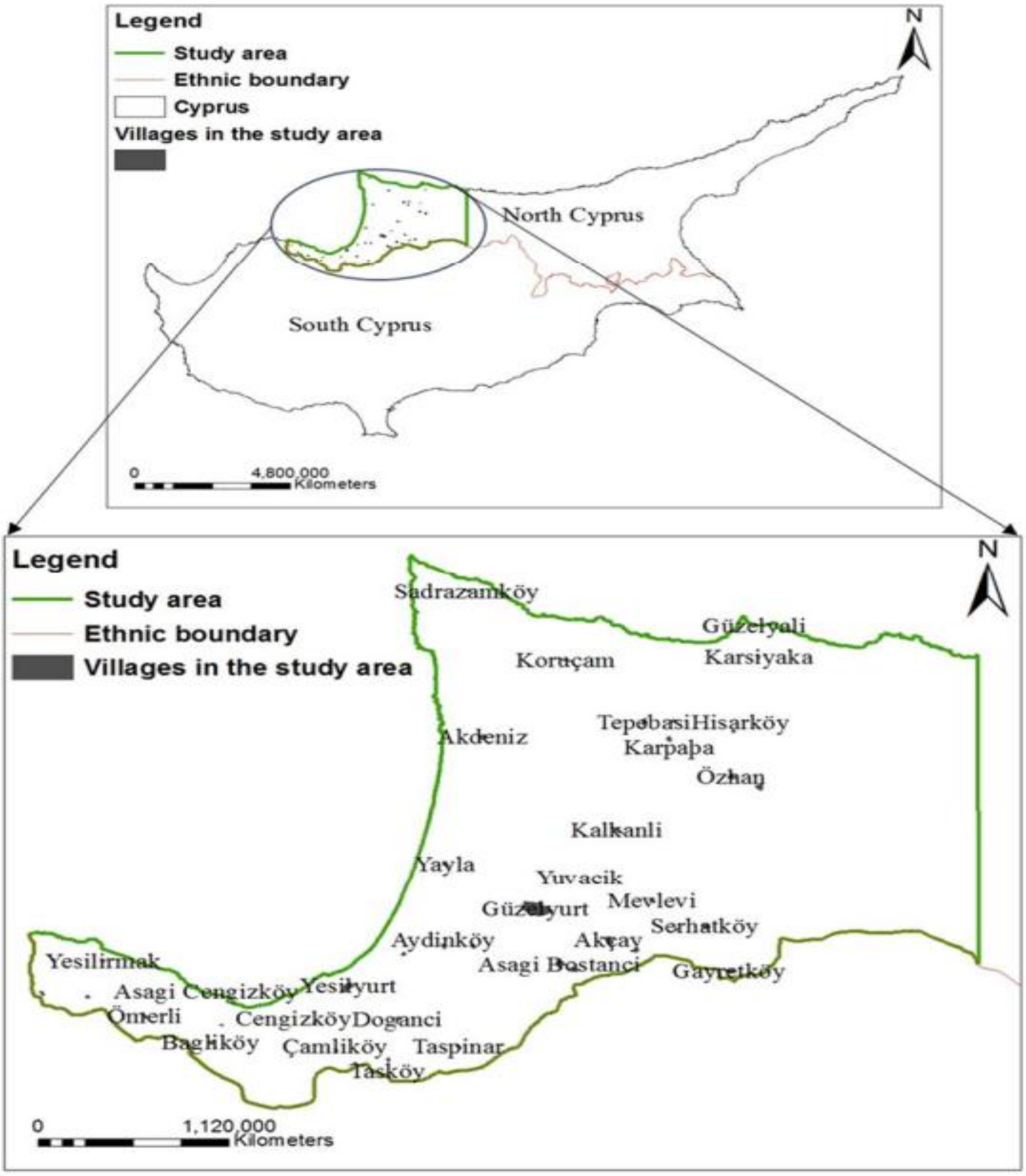

Figure 2.3: Güzelyurt aquifer location in North Cyprus (Gökçekuş and Nourani, 2018)

The Güzelyurt aquifer, which is the largest coastal aquifer in the northwestern of the island, provides water not only for irrigation requirements in the region but also for the municipal needs of Lefkoşa and Gazimağusa cities. According to Gökçekus and Doyuran (1995), the capacity of the Güzelyurt aquifer is found to be 920million cubic meters and recent studies demonstrate that the aquifer has is depleted and the average groundwater level reaches 70 meters below the mean sea level in some local areas (Gökçekus and Kassem 2020). The second important aquifer is the Mount Aquifer, which runs across the northern coast of the island with a thin strip of 1.5 km wide. The surface of this underground reservoir is about 40 km2, with an average annual renewal of 10.5 million cubic meters areas (Gökçekus and Kassem 2020). At the watershed of the Güzelyurt groundwater basin various lithological units of the Troodos massif (middle-Upper Cretaceous), Lapathos group (Oligocene-Lower Miocene), Dhali Group (Middle-Upper Miocene), and Mesaoria Group (Upper Miocene-Upper Pliocene) constitute the bedrock (Gökçekuş 1990). The basin itself comprises flanglomerates (Plestocene) and Holocene deposits.

The Pre-Tertiary Troodos Massif rocks are the oldest units exposed within the watersheds of the Güzelyurt groundwater basin (Searle and Panayiotou 1980). In general, the Troodos Massif is a huge igneous body, which is exposed in the central part of Cyprus. It is made up of Troodos Plutonic Series, Sheeted Dyke Complex, and Pillow Lava Series (Gass and Masson-Smith 1963).

2.2 Agriculture potential and water quality

The production of agriculture is an essential sector in the economy of the Northern part of Cyprus (Payab and Türker 2019; Giannakis et al. 2020). The total agricultural land in the Northern Cyprus is about 187069 ha and the total area equipped for irrigation is about 9.714 ha. Generally, agricultural production share in GDP has been decreased over the year in Cyprus (Papadopoulou et al. 2020). Agricultural water scarcity is more related to the variability of rainfall and access to water resources. According to Park (2020), the annual rainfall in most regions Northern part of Cyprus is within the range of 250-400 mm while Girne (Kyrenia) has the maximum annual amount of rainfall with a value of 583mm. However, the lack of insufficient water resources and dependence on rainwater for irrigation has reduced the production of agriculture yield (Mason 2020; Dodd 1993). Furthermore, agricultural withdrawal accounts for about 75% of the total water withdrawals in Northern Cyprus according to Kahramanoğlu et al. (2020). Also, drought and salinization problems are serious problems for Northern Cyprus since 1970 (Kahramanoğlu et al. 2020). When considering irrigated land, it is noteworthy that over 48% of the total irrigated land is currently devoted to citrus production, 24% to vegetables and greenhouses, 20% to other fruits, and 2% to legumes (Kahramanoğlu et al. 2020). Northern Cyprus's main crop is Almond. Apricot, Banana, Carob, Fig, Grape, Grapefruit, Lemon, Loquat, Mandarine, Olive, Peach, Pear, Plum, Pomegranate, Walnut, and Valencia orange.

According to Gökçekuş et al. 2002, the activities of agriculture in Northern Cyprus are mainly carried in the Güzelyurt region. Agriculture is a major economic activity in Güzelyurt region (Yıldırım et al. 2020). Hence, the region has a high potential for both production and consumption compared to other regions in Northern Cyprus (Arslan and Akün 2019). Güzelyurt region has a large expanse of agricultural land suitable for crop production (Ergil 2000). However, the Güzelyurt state faces significant water challenges (Payab et al. 2020). The agriculture in the Güzelyurt region is divided into two farming systems, namely rainfed agriculture (agriculture that relies on natural rains) and irrigated farming systems.

According to Gökçekuş and Nourani (2018), Citrus fruits constitute the major agricultural product in the Guzelyurt basin, which compares about (70%) of the total production. Also, the most extensive aquifer in Northern Cyprus is located in the Güzelyurt area. Due to seawater intrusion, the physical, chemical, and microbiological properties of aquifer quality have changed. Based on the studies carried by Gökçekuş and Doyuran (1997) and Arslan and Akün (2019) related to evaluating the domestic and agricultural quality of Güzelyurt Basin, it is found that the groundwater samples have high levels of salinity and classified as “hard to very hard” and “slightly alkaline to alkaline”. The effect of climate change on water resources in the region should be addressed in terms of its relation to the water cycle, water pollution, water scarcity, poor water administration, lack of resources for research and technological development, and lack of environmental planning. Additionally, the agriculture in Güzelyurt is expected to increase by helping the water pipe-line from Turkey. Consequently, despite government efforts to extend funding and technical assistance to the farmers, there is still a need to increase the productivity of the agricultural sector.

CHAPTER 3
MATERIAL AND METHODS

3.1 Analysis Procedure

In this section, the potential of solar energy and wind energy in Güzelyurt region are presented. Also, small-scale RO desalination system is designed with various flow rates for agriculture and domestic purposes. Furthermore, the technical, environmental and economic aspects for construction grid-connected solar/wind system in the selected region are presented. A flowchart given in Figure 3.1 illustrates the analysis procedure of this study.

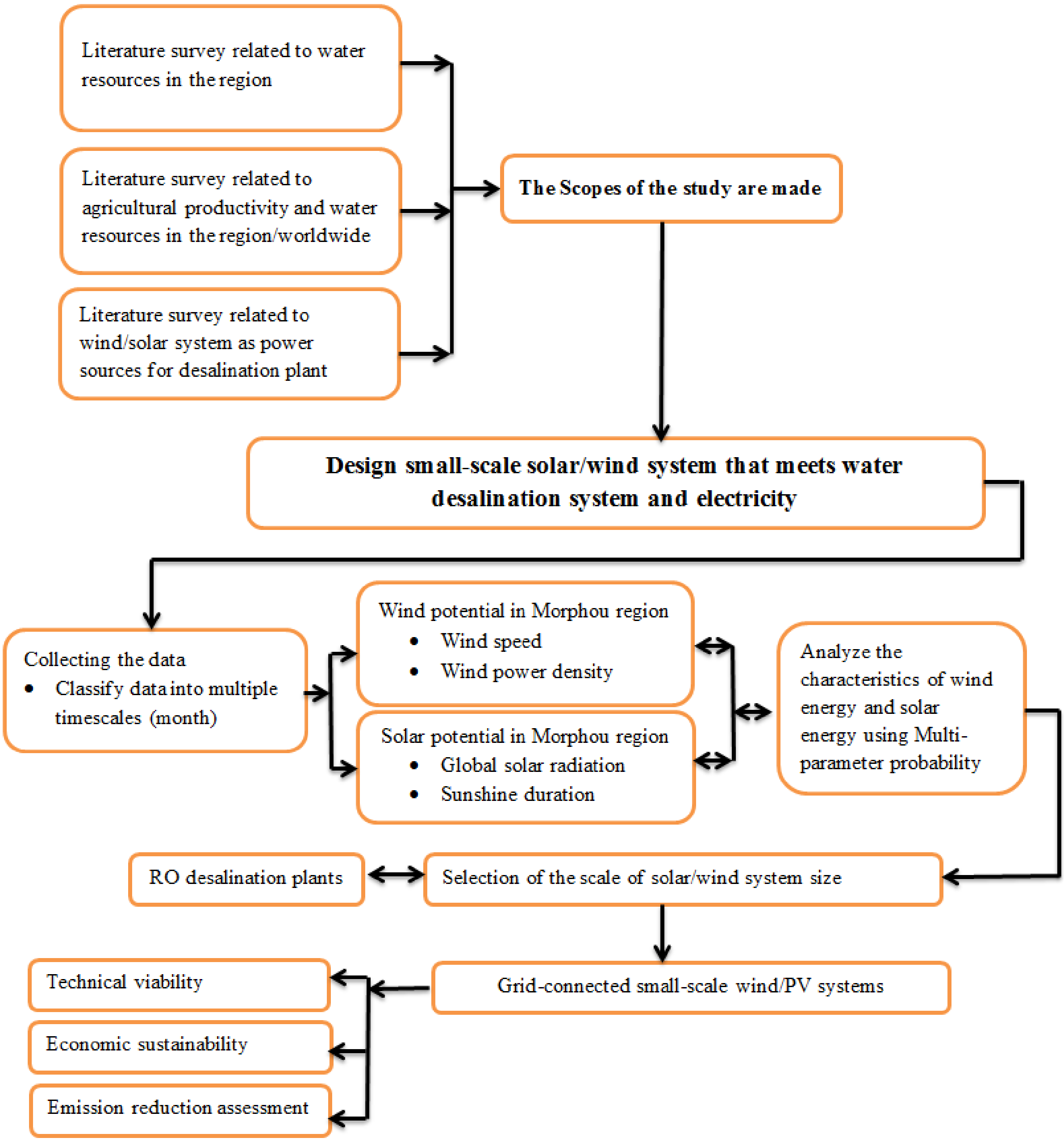

Figure 3.1: Schematic description for the proposed methodology

3.2 Data and Study Area

Figure 3.2 shows the location of the selected region. In this study, the monthly measurement data including average temperature, minimum and maximum temperatures, solar radiation, sunshine duration and wind speed were collected from the Meteorological department located in North Nicosia (Lefkoşa) during 1985–2017. The data were measured at various heights. A cup anemometer device was used to measure the wind speed at 10m height. Additionally, the actinography and thermometer devices were used to measure the solar radiation and temperature at a height of 2m above the ground, respectively.

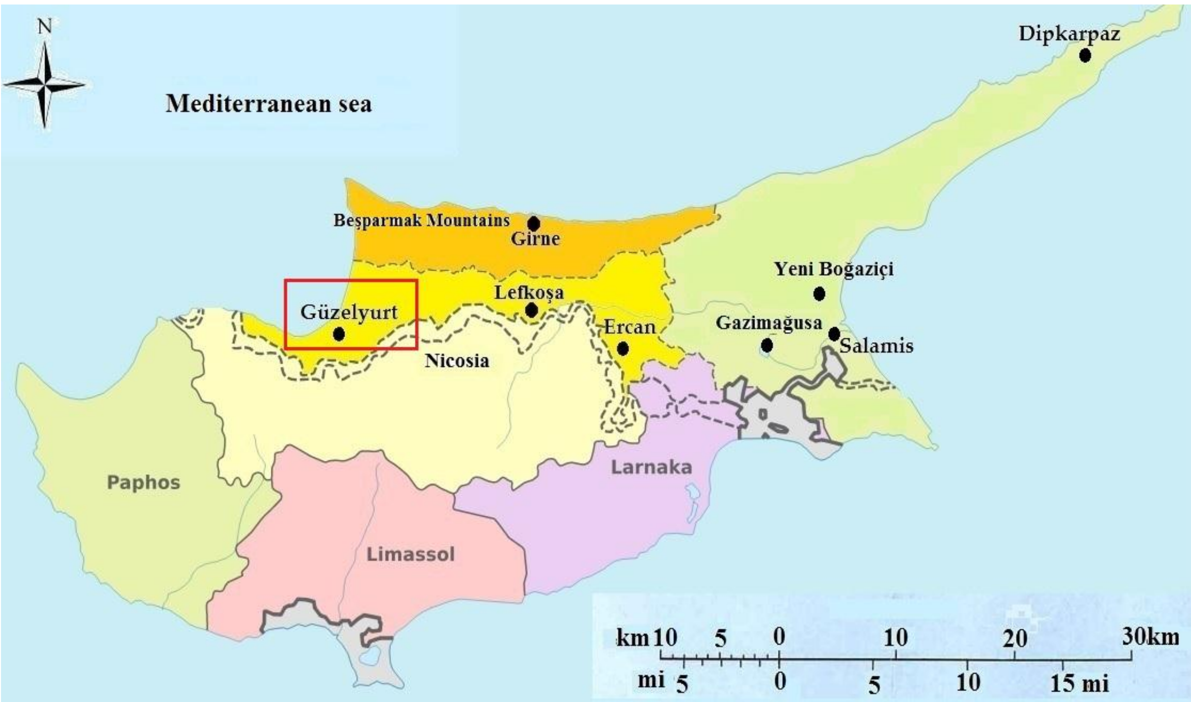

Figure 3.2: The geographical location of Güzelyurt, Northern Cyprus

3.3 Wind Energy Analysis Procedure

3.3.1 Multi-parameter probability distributions for wind speed characterizes

Several scientific studies have investigated the characteristics of wind speed using various distribution functions. For instance, Alayat et al. (2018) utilized ten distribution functions to analyze the characteristic of wind speed in eight selected regions in Northern Cyprus. The results showed that the three-parameter Generalized Extreme Value distribution provided the best fit to the actual data for most regions in Northern Cyprus.

Kassem et al. (2019) analyzed the distribution of wind speed in three coastal regions in Lebanon using ten distribution functions. The results indicated that a two-parameter Log-logistic was considered as the best distribution function to study the wind speed for all selected regions.

Khan et al. (2019) used various distribution functions to analyze the characteristics of wind speed on seven locations in Pakistan. The results showed that three-parameter Generalized Extreme Value distribution was able to provide the best fit to the actual data for the most regions.

Alavi et al. (2016) utilized eight distribution functions for estimating wind speed distribution at five stations in Iran. The results showed that Nakagami and Weibull were selected for modeling wind speed in the selected stations.

Masseran et al. (2015) studied the wind speed characteristics in Peninsular Malaysia using Weibull, Gamma and Inverse Gamma distribution function. It is found that Gamma and Weibull were considered as the best distribution functions to study the wind energy potential in the selected region.

Ouarda et al. (2015) used parametric models, mixture models and one non-parametric model for the evaluation of wind energy potential in United Arab Emirates. The results showed that Kappa and Generalized Gamma distributions provided the best fit to the actual data for all selected stations.

Based on previous scientific studies, it can be concluded that the used distribution function for analyzing the wind speed characteristics are two-parameter Weibull, three-parameter Weibull, Gamma, Lognormal, three-parameter lognormal, Logistic, Log-Logistic, two-parameter Inverse Gaussian, three-parameter Generalized Extreme Value, two-parameter Nakagami, two-parameter Normal, one-parameter Rayleigh, generalized Gamma distribution, exponential, and Kappa distributions.

In this study, 37 distribution functions are used to study the characteristic of wind speed in the selected region (see Table 3.1). The method of maximum-likelihood is utilized to estimate the parameters of distribution models.

Table 3.1: Probability density and cumulative Distribution of used distribution functions

Distribution function	Probability Density Function	Cumulative Distribution Function
Beta	$f(R) = \frac{1}{B(\alpha_1,\alpha_2)} \frac{(R-a)^{\alpha_1-1}(b-R)^{\alpha_2-1}}{(b-a)^{\alpha_1+\alpha_2-1}}$	$F(R) = I_z(\alpha_1,\alpha_2)$
Four-Parameter Burr	$f(R) = \frac{\alpha k \left(\frac{R-\gamma}{\beta}\right)^{\alpha-1}}{\beta\left(1+\left(\frac{R-\gamma}{\beta}\right)^{\alpha}\right)^{k+1}}$	$F(R) = 1-\left(1+\left(\frac{R-\gamma}{\beta}\right)^{\alpha}\right)^{-k}$
Three-Parameter Burr	$f(R) = \frac{\alpha k \left(\frac{R}{\beta}\right)^{\alpha-1}}{\beta\left(1+\left(\frac{R}{\beta}\right)^{\alpha}\right)^{k+1}}$	$F(R) = 1-\left(1+\left(\frac{R}{\beta}\right)^{\alpha}\right)^{-k}$
Cauchy	$f(R) = \left(\pi\sigma\left(1+\left(\frac{R-\mu}{\sigma}\right)^2\right)\right)^{-1}$	$F(R) = \frac{1}{\pi} arctan\left(\frac{R-\mu}{\sigma}\right) + 0.5$
Four-Parameter Dagum	$f(R) = \frac{\alpha k \left(\frac{R-\gamma}{\beta}\right)^{\alpha k-1}}{\beta\left(1+\left(\frac{R-\gamma}{\beta}\right)^{\alpha}\right)^{k+1}}$	$F(R) = 1-\left(1+\left(\frac{R-\gamma}{\beta}\right)^{-\alpha}\right)^{-k}$
Three-Parameter Dagum	$f(R) = \frac{\alpha k \left(\frac{R}{\beta}\right)^{\alpha k-1}}{\beta\left(1+\left(\frac{R}{\beta}\right)^{\alpha}\right)^{k+1}}$	$F(R) = 1-\left(1+\left(\frac{R}{\beta}\right)^{-\alpha}\right)^{-k}$
Three-Parameter Erlang	$f(R) = \frac{(R-\gamma)^{m-1}}{\beta^m\Gamma(m)} exp\left(-\frac{R-\gamma}{\beta}\right)$	$F(R) = \frac{\Gamma_{(R-\gamma)/\beta}(m)}{\Gamma(m)}$
Two-Parameter Erlang	$f(R) = \frac{(R-\gamma)^{m-1}}{\beta^m\Gamma(m)} exp\left(-\frac{R}{\beta}\right)$	$F(R) = \frac{\Gamma_{(R)/\beta}(m)}{\Gamma(m)}$
Two-Parameter Exponential	$f(R) = \lambda\, exp(-\lambda(R-\gamma))$	$F(R) = 1-\ exp(-\lambda(R-\gamma))$
One-Parameter Exponential	$f(R) = \lambda\, exp(-\lambda R)$	$F(R) = 1-\ exp(-\lambda R)$
Three-Parameter Gamma	$f(R) = \frac{(R-\gamma)^{\alpha-1}}{\beta^\alpha\Gamma(\alpha)} exp\left(-\left(\frac{R-\gamma}{\beta}\right)\right)$	$F(R) = \frac{\Gamma_{(R-\gamma)/\beta}(\alpha)}{\Gamma(\alpha)}$
Two-Parameter Gamma	$f(R) = \frac{R^{\alpha-1}}{\beta^\alpha\Gamma(\alpha)} exp\left(-\left(\frac{R}{\beta}\right)\right)$	$F(R) = \frac{\Gamma_{R/\beta}(\alpha)}{\Gamma(\alpha)}$
Generalized Extreme Value	$f(R) = \begin{cases} \frac{1}{\sigma} exp\left(-\left(1+k\frac{R-\mu}{\sigma}\right)^{-1/k}\right)\left(1+k\frac{R-\mu}{\sigma}\right)^{-1-1/k} & k \neq 0 \\ \frac{1}{\sigma} exp\left(-\frac{R-\mu}{\sigma} - exp\left(-\frac{R-\mu}{\sigma}\right)\right) & k = 0 \end{cases}$	$F(R) = \begin{cases} exp\left(-\left(1+k\frac{R-\mu}{\sigma}\right)^{-1/k}\right) & k \neq 0 \\ exp\left(-exp\left(-\frac{R-\mu}{\sigma}\right)\right) & k = 0 \end{cases}$
Four-Parameter Generalized Gamma	$f(R) = \frac{k(R-\gamma)^{k\alpha-1}}{\beta^{k\alpha}\Gamma(\alpha)} xp\left(-\left(\frac{R-\gamma}{\beta}\right)^k\right)$	$F(R) = \frac{\Gamma_{((R-\gamma)/\beta)^k}(\alpha)}{\Gamma(\alpha)}$
Three-Parameter Generalized Gamma	$f(R) = \frac{k(R)^{k\alpha-1}}{\beta^{k\alpha}\Gamma(\alpha)} xp\left(-\left(\frac{R}{\beta}\right)^k\right)$	$F(R) = \frac{\Gamma_{((R)/\beta)^k}(\alpha)}{\Gamma(\alpha)}$

Table 3.1: Continued

Distribution function	Probability Density Function	Cumulative Distribution Function
Generalized Logistic	$f(R) = \begin{cases} \dfrac{\left(1+k\frac{R-\mu}{\sigma}\right)^{-1-1/k}}{\sigma\left(\left(1+k\frac{R-\mu}{\sigma}\right)^{-1/k}\right)^2} & k \neq 0 \\ \dfrac{\exp\left(-\frac{R-\mu}{\sigma}\right)}{\sigma\left(1+\exp\left(-\frac{R-\mu}{\sigma}\right)\right)^2} & k = 0 \end{cases}$	$F(R) = \begin{cases} \dfrac{1}{\left(1+k\frac{R-\mu}{\sigma}\right)^{-1/k}} & k \neq 0 \\ \dfrac{1}{1+\exp\left(-\frac{R-\mu}{\sigma}\right)} & k = 0 \end{cases}$
Generalized Pareto	$f(R) = \begin{cases} \frac{1}{\sigma}\left(-\left(1+k\frac{R-\mu}{\sigma}\right)^{-1-1/k}\right) & k \neq 0 \\ \frac{1}{\sigma}exp\left(-\frac{R-\mu}{\sigma}\right) & k = 0 \end{cases}$	$F(R) = \begin{cases} 1-\left(1+k\frac{R-\mu}{\sigma}\right)^{-1-1/k} & k \neq 0 \\ 1-exp\left(-\frac{R-\mu}{\sigma}\right) & k = 0 \end{cases}$
Maximum Extreme Value Type 1	$f(R) = \frac{1}{\sigma}exp\left(-\frac{R-\mu}{\sigma} - exp\left(-\frac{R-\mu}{\sigma}\right)\right)$	$F(R) = exp\left(-exp\left(-\frac{R-\mu}{\sigma}\right)\right)$
Minimum Extreme Value Type 1	$f(R) = \frac{1}{\sigma}exp\left(\frac{R-\mu}{\sigma} - exp\left(-\frac{R-\mu}{\sigma}\right)\right)$	$F(R) = 1 - exp\left(-exp\left(-\frac{R-\mu}{\sigma}\right)\right)$
Three-Parameter Inverse Gaussian	$f(R) = \sqrt{\frac{\lambda}{2\pi(R-\gamma)}}exp\left(-\frac{\lambda(R-\gamma-\mu)^2}{2\mu^2(R-\gamma)}\right)$	$F(R) = \Phi\left(\sqrt{\frac{\lambda}{R-\gamma}}\left(\frac{R-\gamma}{\mu}-1\right)\right) + \Phi\left(-\sqrt{\frac{\lambda}{R-\gamma}}\left(\frac{R-\gamma}{\mu}+1\right)\right)exp\left(\frac{2\lambda}{\mu}\right)$
Log-Gamma	$f(R) = \frac{\left(ln(R)\right)^{\alpha-1}}{R\beta^{\alpha}\Gamma(\alpha)}exp\left(\frac{-ln(R)}{\beta}\right)$	$F(R) = \frac{\Gamma_{(ln(R)/\beta)^k}(\alpha)}{\Gamma(\alpha)}$
Logistic	$f(R) = \frac{exp\left(-\frac{R-\mu}{\sigma}\right)}{\sigma\left\{1+exp\left(-\frac{R-\mu}{\sigma}\right)\right\}^2}$	$F(R) = \frac{1}{1+exp(-R)}$
Two-Parameter Inverse Gaussian	$f(R) = \sqrt{\frac{\lambda}{2\pi(R-\gamma)}}exp\left(-\frac{\lambda(R-\mu)^2}{2\mu^2 R}\right)$	$F(R) = \Phi\left(\sqrt{\frac{\lambda}{R-\gamma}}\left(\frac{R}{\mu}-1\right)\right) + \Phi\left(-\sqrt{\frac{\lambda}{R-\gamma}}\left(\frac{R}{\mu}+1\right)\right)exp\left(\frac{2\lambda}{\mu}\right)$

Table 3.1: Continued

Distribution function	Probability Density Function	Cumulative Distribution Function
Log-Logistic	$f(R) = \left(\left(\frac{\beta}{\alpha}\left(\frac{R}{\alpha}\right)^{\beta-1}\right) \Big/ \left(1+\frac{R}{\alpha}\right)^{\beta} \right)^{2}$	$F(R) = \frac{1}{\left(1+\frac{R}{\alpha}\right)^{-\beta}}$
Three-Parameter Lognormal	$f(R) = \frac{1}{(R-\gamma)\sigma\sqrt{2\pi}} exp\left[-\frac{1}{2}\left(\frac{ln(R-\gamma)-\mu}{\sigma}\right)^{2}\right]$	$F(R) = \Phi\left[\frac{ln(R-\gamma)-\mu}{\sigma}\right]$
Two-Parameter Lognormal	$f(R) = \frac{1}{R\sigma\sqrt{2\pi}} exp\left[-\frac{1}{2}\left(\frac{ln(R)-\mu}{\sigma}\right)^{2}\right]$	$F(R) = \frac{1}{2} + erf\left[\frac{ln(R)-\mu}{\sigma\sqrt{2}}\right]$
Log-Pearson 3	$f(R) = \frac{1}{R\lvert\beta\rvert\Gamma(\alpha)}\left(\frac{ln(R)-\gamma}{\beta}\right)^{\alpha-1} exp\left(-\frac{ln(R)-\gamma}{\beta}\right)$	$F(R) = \frac{\Gamma_{(ln(R)-\gamma)/\beta}(\alpha)}{\Gamma(\alpha)}$
Nakagami	$f(R) = \frac{2m^{m}}{\Gamma(m)\Omega^{m}} R^{2m-1} e^{\left(-\frac{m}{\Omega}G^{2}\right)}$	$F(R) = \frac{\gamma\left(m, \frac{m}{\Omega}R^{2}\right)}{\Gamma(m)}$
Normal	$f(R) = \frac{1}{\sqrt{2\pi\sigma^{2}}} exp\left(-\frac{R-\mu}{2\sigma^{2}}\right)$	$F(R) = \frac{1}{2}\left[1 + erf\left(\frac{R-\mu}{\sigma\sqrt{2}}\right)\right]$
Two-Parameter Rayleigh	$f(R) = \frac{R-\gamma}{\sigma^{2}} exp\left(-\frac{1}{2}\left(\frac{R-\gamma}{\sigma}\right)^{2}\right)$	$F(R) = 1 - exp\left(-\frac{1}{2}\left(\frac{R-\gamma}{\sigma}\right)^{2}\right)$
One-Parameter Rayleigh	$f(R) = \frac{R}{\sigma^{2}} exp\left(-\frac{1}{2}\left(\frac{R}{\sigma}\right)^{2}\right)$	$F(R) = 1 - exp\left(-\frac{1}{2}\left(\frac{R}{\sigma}\right)^{2}\right)$
Wakeby	$R(F) = \xi + \frac{\alpha}{\beta}\left(1-(1-F)^{\beta}\right) - \frac{\gamma}{\delta}\left(1-(1-F)^{\delta}\right)$	
Three-Parameter Weibull	$f(R) = \left(\frac{\alpha}{\beta}\right)\left(\frac{R-\gamma}{\beta}\right)^{\alpha-1} exp\left(-\left(\frac{R-\gamma}{\beta}\right)^{\alpha}\right)$	$F(R) = 1 - exp\left(-\left(\frac{R-\gamma}{\beta}\right)^{\alpha}\right)$
Two-Parameter Weibull	$f(R) = \left(\frac{\alpha}{\beta}\right)\left(\frac{R}{\beta}\right)^{\alpha-1} exp\left(-\left(\frac{R}{\beta}\right)^{\alpha}\right)$	$F(R) = 1 - exp\left(-\left(\frac{R}{\beta}\right)^{\alpha}\right)$

3.3.2 Goodness-of-Fit test

In order to check the validity of the specified probability distribution model, Goodness-of-fit test statistics are utilized. Kolmogorov-Smirnov (K-S) test, the Anderson-Darling (A-D) test, and Chi-squared (C-s) test are the most well-known empirical distribution function tests.

Kolmogorov-Smirnov (K-S) test

$$D = \max_{1 \le i \le n} \left(F(x_i) - \frac{i-1}{n}, \frac{i}{n} - F(x_i) \right) \quad (3.1)$$

Where

$$F_n(x) = \frac{1}{n} \times (Number\ of\ observation \le x) \quad (3.2)$$

Anderson-Darling (A-D) test

$$A^2 = -n - \frac{1}{n} \sum_{i=1}^{n} (2i-1) \times \left[lnF_X(x_i) + ln\left(1 - F_X(x_{n-i+1})\right) \right] \quad (3.3)$$

where

$F_X(x_i)$ is the cumulative distribution function of the proposed distribution at x_i, for *i* = 1, 2, . . . , *n*.

Chi-squared (C-s) test

$$\mathcal{X}^2 = \sum_{i=1}^{k} \frac{(O_i - E_i)^2}{E_i} \quad (3.4)$$

where O_i is the observed frequency for bin i, and E_i is the expected frequency for bin i calculated by

$$E_i = F(x_2) - F(x_1) \quad (3.5)$$

where F is the cumulative distribution function of the probability distribution being tested, and x_1, x_2 are the limits for bin *i*.

3.3.3 Estimation of wind turbine energy output

The wind power density (WPD) indicates the how much energy is available at the region that needs for converting it to electricity by using a wind turbine. It is the ratio between the wind power (P) and area (A) and it can be estimated using Eqs. (3.6) and (3.7).

$$\frac{P}{A} = \frac{1}{2}\rho v^3 \tag{3.6}$$

$$\frac{P}{A} = \frac{1}{2}\rho v^3 f(v) \tag{3.7}$$

Furthermore, the average WPD can be determined using Eq. (3.8)

$$\frac{\bar{P}}{A} = \frac{1}{2}\rho \bar{v}^3 \tag{3.8}$$

where P is wind power density in W, $\bar{P}$ is mean wind power density in W, A is swept area in m^2, ρ is the air density in kg/m^3, $f(v)$ is the probability density function (PDF), and $\bar{v}$ is the mean wind speed in m/s.

The percentage of errors in estimating the wind power density is calculated as follows

$$Error = \left| \frac{\left(\frac{P}{A}\right)_{estimated} - \left(\frac{P}{A}\right)_{actual}}{\left(\frac{P}{A}\right)_{actual}} \right| \times 100\% \tag{3.9}$$

Moreover, the ratio of the actual energy output (E_{out}) in a period to the theoretical maximum output (E_r) is called the capacity factor (C_f). It can be expressed as follow

$$C_f = \frac{E_{out}}{E_r} \tag{3.10}$$

3.4 Solar energy analysis procedure

In this section, the methodology that is considered for the proposed solar PV plants in the selected region is discussed. In general, power generation depends on the capacity of the PV system (number of PV modules). In the present study, grid-connected solar PV systems are proposed for generating enough energy to power the residential buildings and RO desalination plant in the coastal region in Northern Cyprus. It should be noted that the sun-tracking system, shading or partial shading, dust, and cell operating temperature are the essential parameters that affect the power generation of the PV system (Lau et al. 2017).

According to Kassem et al. (2020), the important parameters that are considered for designing a PV solar plant are defined as follows

Power generating factor (PGF)

$$PGF = \frac{SI \times SH}{STCI} \tag{3.11}$$

Energy demand (ED)

$$ED = ECAL \tag{3.12}$$

Solar PV energy required (SPVER)

$$SPCER = PER \times ELS \tag{3.13}$$

PV module sizing

$$TWPR = \frac{SPVER}{PGF} \tag{3.14}$$

$$PVMS = \frac{TWPR}{PVOPR} \tag{3.15}$$

Inverter sizing (IS)

$$IS = PER \times FS \tag{3.16}$$

where *SI* is solar irradiance, *SH* is the sunshine hour, *STCI* is standard test condition irradiance, *ECAL* is the energy consumption of all loads, *TWPR* is total watt peak ratting, *SPVER* is solar PV energy required, *PGF* is panel generation factor, *PVMS* is PV module size, *PVOPR* is PV output power rating, *FS* is the factor safety, *PER* is peak energy requirement, *ELS* is energy lost in the system and the factor safety is 1.3

3.5 Design of water desalination system

In order to ensure quality of water for the crops, farmers have selected to finance and install small-scale desalination plant. The saline groundwater from the coastal aquifer is the main source for the desalination plant. Therefore, in order to determine the energy needs from the wind/solar renewable system, the energy required for the RO desalination plant should be estimated. It can be determined using the below equation (Gold and Webber 2015; Fornarelli et al. 2018).

$$P_D = \frac{SEC \cdot q}{CF_D} \tag{3.17}$$

where P_D is power requirement of the RO in kW, CF_D is the capacity factor of the plant ($CF_D = 95\%$ (Gold and Webber 2015), q is the flow rate for the feed water in m^3/h and SEC is the specific energy consumption of desalination in kWh/m^3 (it is varied between 0.5 and 3 kWh/m^3 (Semiat 2008; Siddiqi and Anadon 2011; Gold and Webber 2015; Fornarelli et al. 2018).

In the present study, the value of SEC is assumed to be 1.5 kWh/m^3, which is the average value of 0.5-3 kWh/m^3 range given in the literature (Semiat 2008; Siddiqi and Anadon 2011; Gold and Webber 2015; Fornarelli et al. 2018). Also, it is assumed the flow rate is 15000L/day (15m^3/day) that referred to the constant capacity operation of the RO plant.

CHAPTER 4
RESULTS AND DISCUSSION

4.1 Wind Energy Potential

The descriptive statistics including mean, maximum, minimum, standard deviation (SD), coefficient of variation (CV), skewness, and kurtosis of each region are presented in Table 4.1. It is observed that the mean wind speed is within the range of 3.424-1.325m/s. The maximum and minimum wind speed values are recorded in July 1981 and February 1990, respectively. The variation coefficients are moderately high, ranging from 9.43 to 41.44 as shown in Table 4.1.

Table 4.1: Descriptive statistics of wind speed data at 10m

Year	Mean	SD	CV	Min.	Max.	Skewness	Kurtosis
1981	2.12	0.844	39.82	0.413	3.294	-0.3	0.09
1982	1.325	0.549	41.44	0.767	2.464	0.97	-0.05
1983	1.685	0.484	28.75	1.013	2.558	0.62	-0.18
1984	1.986	0.781	39.32	0.877	3.5	0.33	-0.28
1985	2.954	1.102	37.32	1.3	4.316	-0.11	-1.59
1986	1.86	0.53	28.5	1.023	2.7	-0.18	-1.05
1987	1.661	0.587	35.34	0.7	2.539	-0.25	-0.89
1988	3.035	0.558	18.38	2.245	3.89	0.18	-1.26
1989	2.794	0.934	33.42	1.1	4.194	-0.78	0.4
1990	3.289	0.608	18.48	2.559	4.814	1.49	2.89
1991	3.424	0.655	19.12	2.497	4.219	-0.37	-1.73
1992	3.287	0.834	25.38	2.2	4.683	0.39	-1.42
1993	3.094	0.73	23.58	2.171	4.629	1.02	0.23
1994	3.019	0.509	16.87	2.339	4.083	0.58	0.32
1995	2.835	0.3341	11.78	2.1857	3.2333	-0.73	-0.43
1996	2.981	0.45	15.11	2.363	3.637	0.34	-1.54
1997	2.982	0.718	24.07	2.119	4.065	0.44	-1.2
1998	2.803	0.801	28.58	1.603	4.126	0.57	-0.61
1999	2.562	0.478	18.66	1.794	3.386	0.12	-0.64
2000	2.531	0.601	23.75	1.8	3.713	0.9	-0.05
2001	2.369	0.45	18.99	1.847	3.355	1.03	0.69
2002	1.931	0.629	32.58	1.119	3.339	1.06	1.17
2003	2.81	0.818	29.13	1.643	4.618	0.78	0.86
2004	2.776	0.543	19.56	1.981	3.872	0.58	-0.12
2005	2.766	0.436	15.75	2.129	3.565	0.63	-0.22
2006	2.706	0.419	15.48	2.177	3.571	0.7	-0.15
2007	2.4368	0.2297	9.43	2.0645	2.8387	0.14	-0.65
2008	2.495	0.456	18.26	1.881	3.5	0.65	0.79
2009	2.4875	0.3018	12.13	1.8742	3.0032	-0.35	0.65
2010	2.416	0.447	18.51	1.567	3.264	0.01	0.56
2011	2.3947	0.2667	11.14	2.0484	2.8533	0.06	-1.31
2012	2.326	0.389	16.72	1.803	3.166	0.88	0.37
2013	2.601	0.404	15.54	2.052	3.384	0.58	-0.11
2014	2.475	0.418	16.89	2	3.2	0.89	-0.6
2015	2.5693	0.3451	13.43	1.9516	3.052	-0.08	-0.7
2016	2.501	0.348	13.93	1.994	3.071	0.11	-0.8
2017	2.431	0.55	22.64	2.027	4.045	2.62	7.8
Mean	2.6547	0.2658	10.01	2.2847	3.1299	0.55	-0.76

Moreover, the annual and monthly wind speed data during the investigation period are shown in Figure 4.1. It is found that the maximum and minimum wind speed values are recorded in 1991 and 1982 with a value of 3.42 and 1.32m/s, respectively.

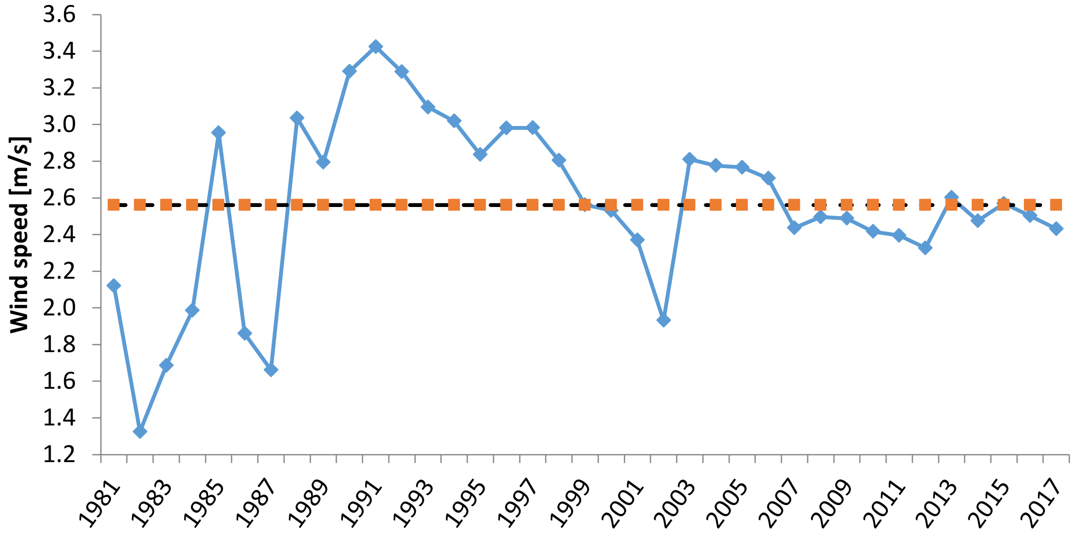

Figure 4.1: Mean annual wind speed during the investigation period

During the investigation period, the highest and lowest values of monthly wind speed are recorded in February (3.1 m/s) and October (2.3 m/s) as shown in Figure 4.2.

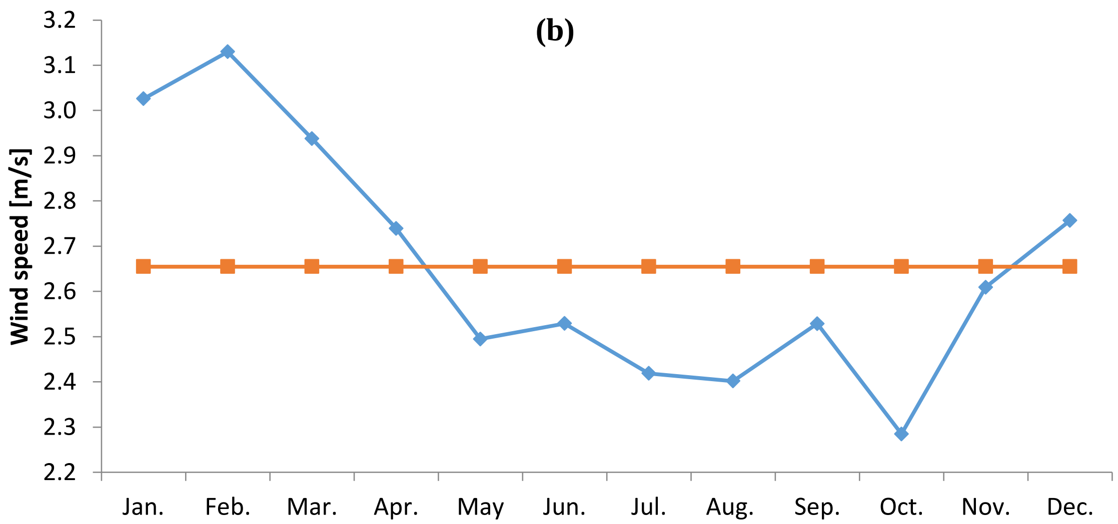

Figure 4.2: Mean annual wind speed during the investigation period

In this study, the monthly wind speed was utilized to identify the characteristics of wind speed of the selected region using the 37 distribution functions. Kolmogorov-Smirnov (K-S) test, Anderson-Darling (A-D) test, and Chi-squared (C-s) test were utilized to select the best distribution among the 37 distribution functions. In general, the lowest value of K-S, A-D, and C-s value will be selected to be the best distribution to analyze the wind speed characteristics. Table 4.2 lists the distribution parameter and the value of K-S, A-D and C-s for average monthly wind speed. Based on the K-S test, Burr (4P) distribution has the lowest value, which considered as the best distribution function to investigate the wind speed characteristics. Also, it is found that Wakeby and Gen. Extreme Value distribution functions are considered as the best model to study the distribution of the wind speed based on A-D and C-s, respectively. Similar result has been by Alayat et al. (2018). The found that Gen. Extreme Value distribution provided the best fit to the actual wind speed data for Güzelyurt region compared to other selected distribution functions (Weibull, Gamma, Lognormal, Logistic, Log-Logistic, Inverse Gaussian, Nakagami, Nakagamia and Rayleigh).The best model, which provided the best fit to the actual data, is presented in Table 4.3. Figure 4.3 illustrates the frequency histograms and probability plots of wind speed.

Table 4.2. Distribution parameters and results of goodness-of-fit tests

Distribution	Parameters	K-S	A-D	C-s
Beta	α_1=0.58185 α_2=0.78053 a=2.3 b=3.1	0.17013	1.8632	0.33395
Burr	k=0.19211 α=49.81 β=2.3823	0.13005	0.2668	0.03030
Burr (4P)	k=127.37 α=1.3101 β=15.381 γ=2.2876	0.12794	0.2698	0.04014
Cauchy	σ=0.14742 μ=2.5378	0.18187	0.7702	0.10935
Dagum	k=104.9 α=17.063 β=1.8908	0.21216	0.8986	0.00016
Dagum (4P)	k=0.28041 α=2.8269 β=0.46745 γ=2.3	0.24792	4.6530	N/A
Erlang	m=105 β=0.02509	0.19172	0.3323	2.05420
Erlang (3P)	m=2 β=0.21163 γ=2.272	0.20730	0.4254	0.09838
Exponential	λ=0.37855	0.58133	4.5638	0.14390
Exponential (2P)	λ=2.9268 γ=2.3	0.19310	2.6417	0.11206
Gamma	α=105.27 β=0.02509	0.20116	0.3406	2.15430
Gamma (3P)	α=1.7468 β=0.21163 γ=2.272	0.12857	0.2511	0.03568
Gen. Extreme Value	k=0.01546 σ=0.21437 μ=2.5146	0.15718	0.2378	0.00006
Gen. Gamma	k=1.0164 α=113.61 β=0.02509	0.21260	0.3863	2.34190
Gen. Gamma (4P)	k=1.6904 α=0.41362 β=0.5036 γ=2.3	0.30717	5.5363	N/A
Gen. Logistic	k=0.1799 σ=0.14286 μ=2.5978	0.17486	0.2868	0.00055
Gen. Pareto	k=-0.39012 σ=0.5009 μ=2.2813	0.13675	0.2153	0.01672
Gumbel Max	σ=0.20074 μ=2.5258	0.17926	0.2767	0.00112
Gumbel Min	σ=0.20074 μ=2.7575	0.25788	0.9356	1.74250
Inv. Gaussian	λ=278.1 μ=2.6417	0.21417	0.3571	2.40850
Inv. Gaussian (3P)	λ=2.11 μ=0.53604 γ=2.1056	0.15144	0.2514	0.01670
Log-Gamma	α=101.78 β=0.0095	0.19391	0.3035	0.23564
Log-Logistic	α=16.433 β=2.5915	0.14347	0.3719	0.10495
Log-Logistic (3P)	α=2.7752 β=0.38737 γ=2.1922	0.15429	0.2604	0.04058
Log-Pearson 3	α=20.862 β=0.02099 γ=0.52929	0.18397	0.2731	0.28454
Logistic	σ=0.14195 μ=2.6417	0.23067	0.4720	2.21960
Lognormal	σ=0.09178 μ=0.96715	0.21026	0.3733	2.43480
Lognormal (3P)	σ=0.49197 μ=-0.75889 γ=2.116	0.15642	0.2553	0.01617
Nakagami	m=25.57 Ω=7.0392	0.19951	0.3463	2.01130
Normal	σ=0.25746 μ=2.6417	0.20892	0.3797	2.03010
Pareto	α=7.4492 β=2.3	0.21266	2.0468	0.39601
Pareto 2	α=218.29 β=575.56	0.58129	4.5640	0.14298
Rayleigh	σ=2.1077	0.44864	3.1272	0.03958
Rayleigh (2P)	σ=0.41051 γ=2.208	0.27648	0.8349	4.21780
Wakeby	α=0.5009 β=0.39012 γ=0 δ=0 ξ=2.2813	0.13675	0.2153	0.01672
Weibull	α=11.345 β=2.7081	0.16788	0.6225	1.07920
Weibull (3P)	α=1.3802 β=0.39094 γ=2.2827	0.14105	0.2597	0.02935

Table 4.3: Best models for studying the characteristics of wind speed

Goodness-of-fit test	Rank				
	1	**2**	**3**	**4**	**5**
K-S	Burr (4P)	Gamma (3P)	Burr	Wakeby	Gen. Pareto
D-A	Wakeby	Gen. Pareto	Gen. Extreme Value	Gamma (3P)	Inv. Gaussian (3P)
C-s	Gen. Extreme Value	Dagum	Gen. Logistic	Gumbel Max	Lognormal (3P)

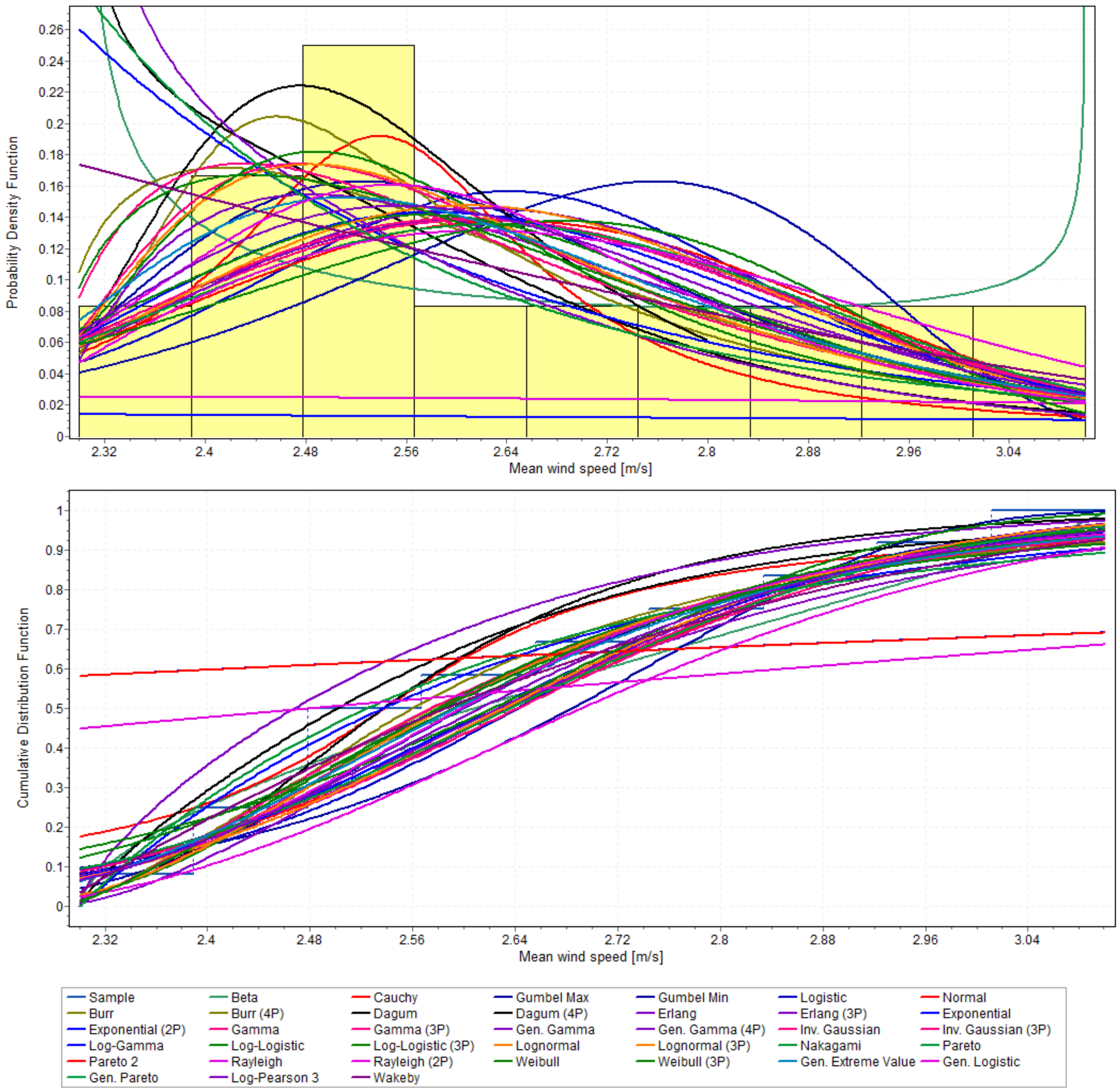

Figure 4.3: Frequency histograms, probability density and cumulative distribution function plots of average monthly wind speed

Furthermore, the wind power density (WPD) value can be regarded as a representative value for the potential of wind energy of a specific location. In this study, the value of air density is assumed to be constant (ρ = 1.23 kg/m3). The estimated value of the average WPD for the selected region is tabulated in Table 4.4. It is found that the value of WPD is around 11W/m^2. According to the average power density values classification, the wind energy generation potential of the selected region is classified as class 1 (poor) (Kassem et al., 2019). Thus, it can be concluded that the high-scale wind turbines are not suitable to generate electricity from wind energy in the selected region. However, the low cut-in wind turbine is considered as a good option to be utilized to produce electricity in the selected regions, which can be installed on the rooftop of a building.

Table 4.4: Parameter values of the best distribution functions at 10 m height

Model	Variable	Value	Model	Variable	Value
Burr (4P)	mean [m/s]	2.6402	Burr	mean [m/s]	2.6471
	Variance	0.0746		Variance	0.1051
	SD [m/s]	0.2732		SD [m/s]	0.3242
	CV	0.1035		CV	0.1225
	Skeweness	1.3598		Skeweness	2.5896
	Kurtosis	2.5255		Kurtosis	13.6010
	WPD [W/m^2]	11.0424		WPD [W/m^2]	11.1292
Wakeby	mean [m/s]	2.6417	Gen. Extreme Value	mean [m/s]	2.6417
	Variance	0.0729		Variance	0.0788
	SD [m/s]	0.2701		SD [m/s]	0.2807
	CV	0.1022		CV	0.1063
	Skeweness	0.7499		Skeweness	-1.2349
	Kurtosis	-0.1992		Kurtosis	2.8862
	WPD [W/m^2]	11.0612		WPD [W/m^2]	11.0612
Gamma (3P)	mean [m/s]	2.6417	Gen. Pareto	mean [m/s]	2.6417
	Variance	0.0782		Variance	0.0729
	SD [m/s]	0.2797		SD [m/s]	0.2701
	CV	0.1059		CV	0.1022
	Skeweness	1.5132		Skeweness	0.7499
	Kurtosis	3.4348		Kurtosis	-0.1992
	WPD [W/m^2]	11.0612		WPD [W/m^2]	11.0612
Dagum	mean [m/s]	2.5759	Lognormal (3P)	mean [m/s]	2.6444
	Variance	0.0414		Variance	0.0765
	SD [m/s]	0.2034		SD [m/s]	0.2765
	CV	0.0790		CV	0.1046
	Skeweness	-		Skeweness	1.7132
	Kurtosis	-		Kurtosis	5.6352
	WPD [W/m^2]	10.2551		WPD [W/m^2]	11.0951
Inv. Gaussian (3P)	mean [m/s]	2.6417	Gumbel Max	mean [m/s]	2.6417
	Variance	0.0730		Variance	0.0663
	SD [m/s]	0.2702		SD [m/s]	0.2575
	CV	0.1023		CV	0.0975
	Skeweness	1.5121		Skeweness	1.1395
	Kurtosis	3.8108		Kurtosis	2.4000
	WPD [W/m^2]	11.0612		WPD [W/m^2]	11.0612

4.2 Solar Energy Potential

In general, solar radiation (SR) is one of the major factors that affect the annual energy exported to the grid by the panel and the capacity factor (Mehmood et al. 2014; Khandelwal and Shrivastava 2017). The variations of average monthly and annual global solar radiation (SR) are illustrated in Figures 4.4. It is found that the monthly solar radiation is varied from 69.98kWh/m^2 to 219.67kWh/m^2 as shown in Figure 4.4(b). The maximum and minimum values of SR are recorded in June and December, respectively. Moreover, it is observed that the highest and lowest values of annual SR are recorded in 2016 and 2009 with a value of 2041.46kWh/m^2 and 1463.63kWh/m^2, respectively.

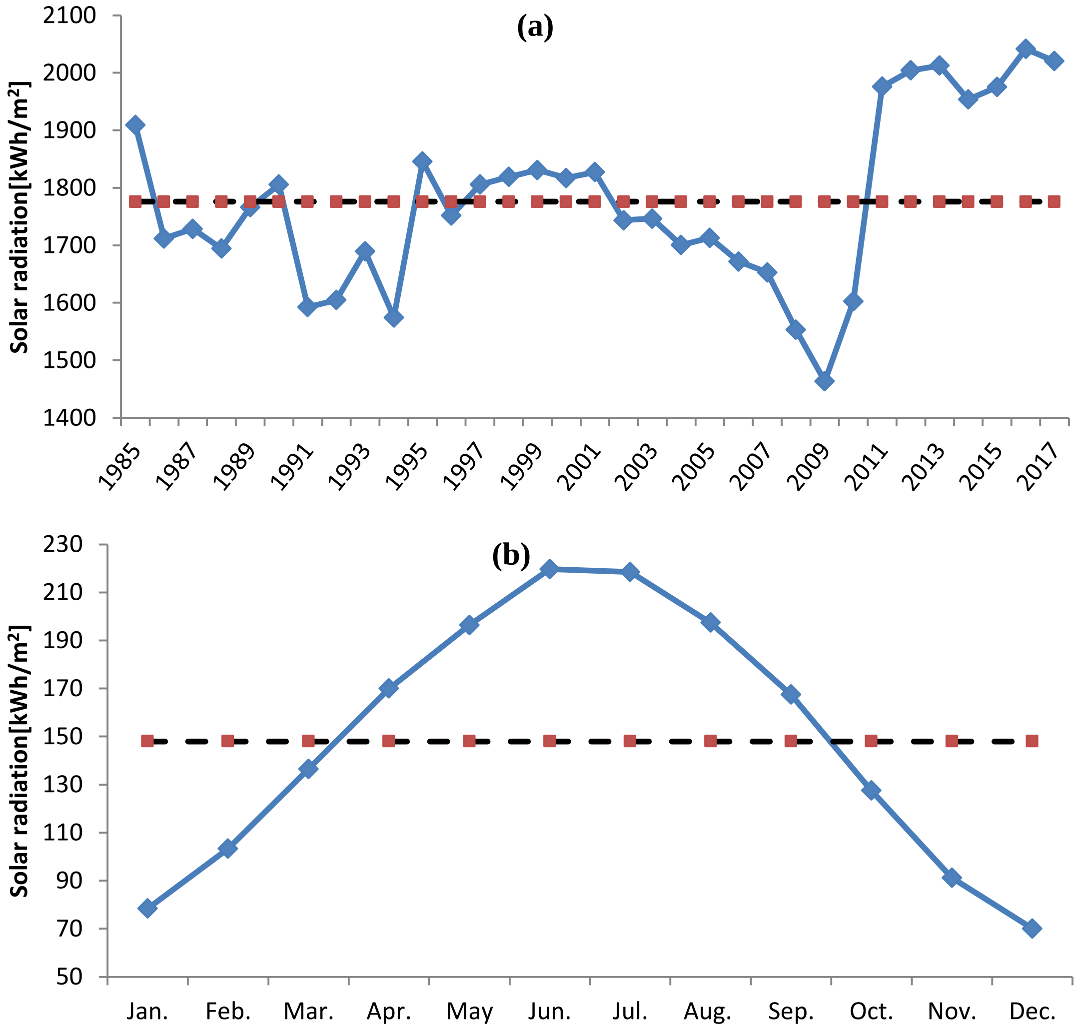

Figure 4.4: Average solar radiation; (a) annual and (b) monthly data

In general, global solar radiation is considered applicable for evaluating the energy generation for the flat PV system. The solar energy potential was classified based on the annual value of global solar radiation (GSR) as shwon in Table 4.5 (Prăvălie et al. 2019). It is found that the solar resource of the selected region is categorized as good (class 4). Thus, this region is a suitable region for installing a PV system in the future due to the high value of GSR.

Table 4.5: Classification of solar energy

Class	**Annual GSR [kWh/m^2]**
1 (Poor)	<1191.8
2 (marginal)	1191.8-1419.7
3 (fair)	1419.7-1641.8
4 (good)	1641.8-1843.8
5 (excellent)	1843.8-2035.9
6 (outstanding)	2035.9-2221.8
7 (superb)	>2221.8

Additionally, the behavior of average annual sunshine duration and air temperature is analyzed for the selected location as shown in Figure 4.5. Based on the data given in Figure 4.5, the average temperature in the selected location was approximately 18.5℃. Also, the sunshine duration during the investigation period ranged between 8.5 and 9.6 h/day as shown in Figures 4.5.

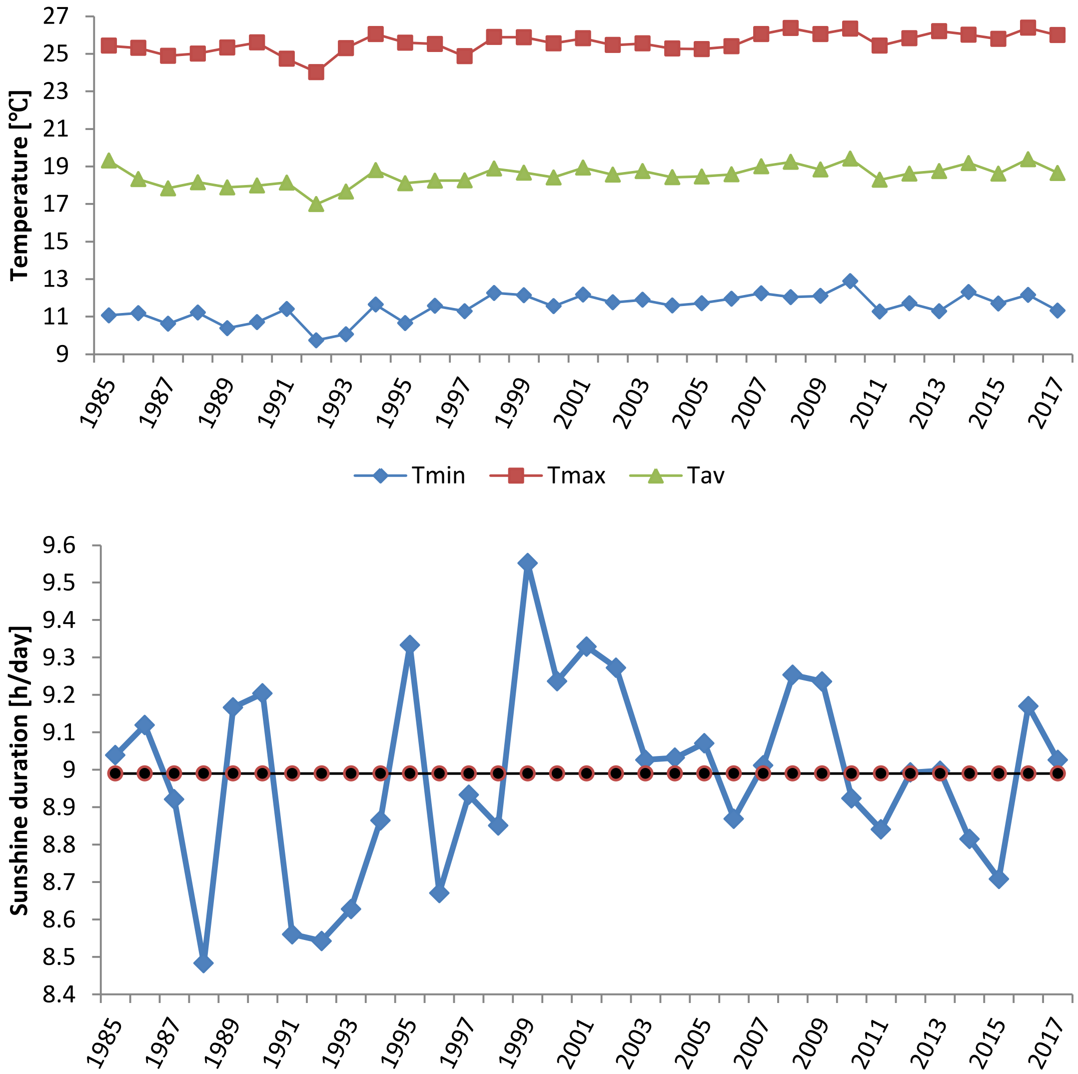

Figure 4.5: Annual air temperature and sunshine duration during the investigation period

4.3 PV system as power source for household and reverse osmosis desalination plant

To ensure sufficient supply from the energy source during the year, the load profile of the household and desalination plant is calculated. This section aims to evaluate the techno-economic performance of small-scale grid-connected PV systems with various sun-tracking systems and PV technologies for a family household. Designing the electrical load is an essential part of this section. The energy demand in the family house is required for different usage. The energy demand (E_{load}) in kW/d of the considering household can be estimated using the given equation.

$$E_{load} = \sum_{j=1}^{N_{category}} P_j n_j T_j \tag{4.1}$$

where P_j is the rated power of the j-th kind of household appliance (kW), T_jNJ is the number of the j-th kind of household appliance, T_j is the used hours per day of the j-th kind of household appliance (h/day) and $N_{Category}$ is the category number of household appliances.

The monthly electrical energy consumptions of the considered household are shown in Figure 4.6 during the period of 2014-2020.

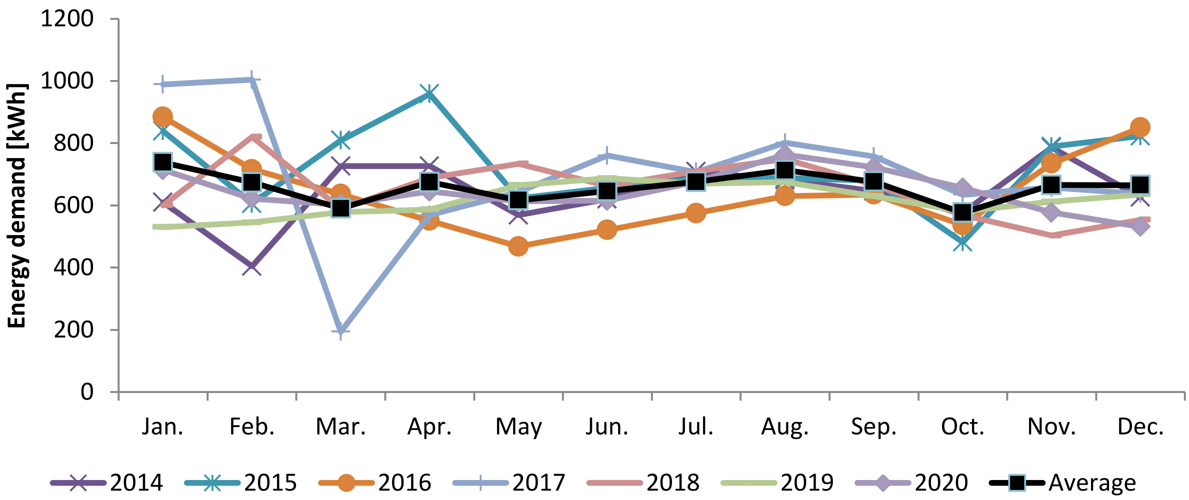

Figure 4.6: Load demand of the household

It is found that the total electricity consumption of the selected household is about 7900kWh/year (i.e. 21.67 kWh/day). Besides, the required power need for the developed RO desalination plant is estimated to be 1kW (see section 2.3). The maximum daily power consumption for the household and RO desalination plant is estimated to be 26kWh/day.

The aim of this section is to design a PV system that able to meet the energetic requirements of the household and RO desalination plant. To be the developed system is feasible, the designed system should respect the annual net energy balance condition (Eq. (4.2)) (Nacer et al. 2016).

$$E_{inj} > E_{abs} \tag{4.2}$$

where E_{inj} is the amount of photovoltaic energy injected into the grid and E_{abs} is the amount of electricity purchased by the system from the grid.

Moreover, the maximum power (P_{max}) of the fixed-tilt PV system can be determined based on the maximum value of global solar radiation (G_{SR}) using Eq. (4.3) (Maammeur et al. 2017).

$$P_{max} = \frac{E_{AC} P_i}{G_{SR} f_{PV} \eta_{inv}} \tag{4.3}$$

where P_i is the solar radiation at STC in kW/m^2, G_{SR} is the global solar radiation (kWh/m^2/d), f_{PV} is the PV derating factor (80%), E_{AC} is the daily power consumption in kWh/d and η_{inv} is the inverter yield (99.9%).

Based on the actual data, it is found that the maximum global solar radiation of 7.32kWh/m^2/day is recorded in June. Using Eq. (4.2), the maximum power of the PV system is found to be 4.53kWh.

A large number of Photovoltaic (PV) modules with different specifications are available in the Turkey and Northern Cyprus market. A selection criterion is needed to select the best Photovoltaic (PV) modules for the proposed PV system design. In general, Mono-crystalline PV modules having the highest efficiency compared to Poly-crystalline cells and amorphous silicon modules. The selection of PV modules depends on the required applications. According to Said et al. (2015), several aspects such as cell type, system cost, the warranty, and the size and watts are widely used to select the best PV modules of different technologies. In this study, The PV modules with an efficiency of less than 15% are not selected. The chosen of the suitable PV-module type was selected based on Eq. (4.4).

$$\text{Panel selection} = \frac{PV\ module\ capacity \times Module\ \text{efficiency}}{module\ price\ \times Frams\ area\ of\ the\ module} \tag{4.4}$$

By using the proposed criterion, it is found that AS-M60-310W made Mono-crystalline, which is manufactured by Ankara Solar was selected. Table 4.6 summarizes the specification of the selected module.

Table 4.6: PV module specification at Standard Test Conditions

Item	**Specification**
Manufacturer	Ankara Solar
Model	AS-M60 310W
Maximum Power (P_{max}) [W]	310
The voltage at Maximum Power (Vmp) [V]	31.7
Current at Maximum Power (Impp) [A]	9.8
Open Circuit Voltage (Voc) [V]	39.7
Short Circuit Current (Isc) [A]	10.12
Operating Temperature Range [℃]	-40~85
Temperature Coefficient of P_{max} [%/℃]	-0.41
Temperature Coefficient of Voc [%/℃]	-0.31
Temperature Coefficient of Isc [%/℃]	0.05
Module Price [$]	77

Moreover, the inverter is a device used to convert the produced DC power from the PV panels to AC power. There are several types of inverters in the market. However, the suitable inverter selection depends on three main factors (output AC power, DC-AC conversion efficiency, capital cost). After an intensive search for a proper inverter choice, two units of central inverters of Sunny Central 850CP XT with a capacity of 954kW and 98.6% efficiency were used. The specification of the selected inverter is available in Ref. (Tanfon Solar).

4.3.1 Technical viability

Figure 4.7 illustrates the monthly average daily global radiation on a horizontal surface and various orientation angles. In general, the optimum angles including slope angle and azimuth angle for the fixed-tilt system are estimated using Photovoltaic Geographical Information System (PVGIS) simulation tool. Several scientific studies have used PVGIS to find the slope angle and azimuth angle for the PV system (Abdallah et al. 2020; Bailek et al., 2018). Generally, the PVGIS provides the optimum slop and azimuth angles that give the maximum annual global solar radiation for a specific location (Abdallah et al. 2020). Therefore, the slop and azimuth angles for selected locations are estimated to be 31° and 2°, respectively. Also, the optimum azimuth angle for vertical axis system is found to be 52°. It is observed that the highest value of solar radiation is obtained from the sun-tracking systems (vertical axis and two axis systems) as shown in Figure 4.7. Also, it is found that the maximum and minimum values of solar radiation are recorded in July and December as shown in Figure 4.7.

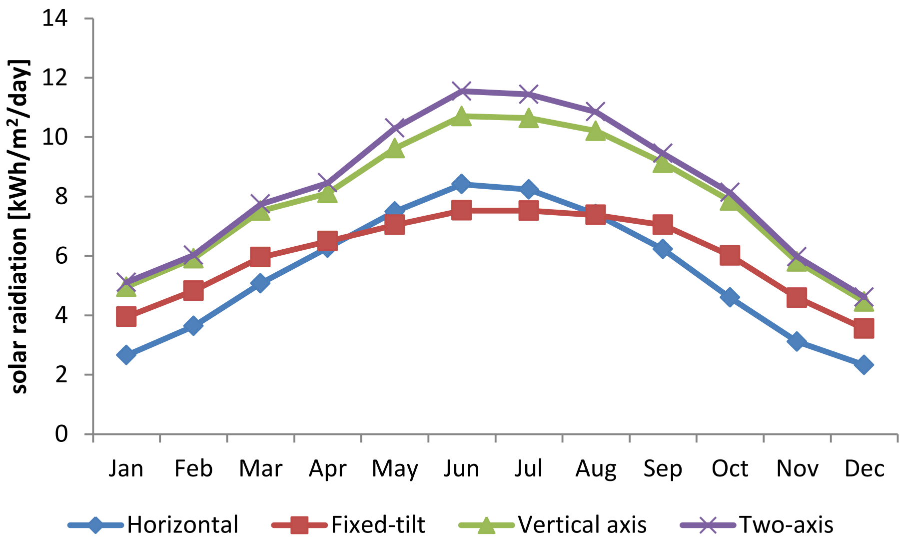

Figure 4.7: Monthly average daily global radiation on a horizontal surface, fixed-titled surface, vertical-axis surface and Two-axis

In this study, the techno-economic analysis of the proposed PV systems (fixed-tilt, vertical axis, and Two-axis system) have been investigated using RETScreen software. According to Mehmood et al. (2014) and Khandelwal and Shrivastava (2017), solar radiation and the number of clear sunny days are important factors that affect the annual energy exported to the grid by the panel and the capacity factor. The monthly electricity generation (EG) from the proposed systems is shown in Table 4.7. It is found that the monthly EG is within the range of 414.84kWh-804.45kWh for fixed-tilt system, 518.14-11545.24kWh for vertical-axis system and 535.48-1218.46kWh for Two-axis PV system. The maximum value of EG is recorded in July for all proposed systems. It can be concluded that the amount of output power could be increased by 51.46% and 43.60% when the Two-axis and vertical-axis sun trucking system are used. Besides, it is found that the capacity factor (CF) values of all developed systems is 19.27, 25.58 and 26.60% for fixed-tilt, vertical axis, and Two-axis system, respectively as shown in Table 4.7. These observations can be supported by other scientific researchers who analyzed the feasibility of a grid-connected PV system. For instance, Kazem and Khatib (2012) found that the CF of the proposed PV system in Oman was within the range of 16-23%. Also, Obeng et al. (2020) found that the CF of grid-connected PV systems with various technologies was varied from 15.37% to 15.75%. Moreover, Mohammadi et al. (2018) found that the value of CF of grid-connected PV systems with different sun-tracking modes was within the range of 17.54-27.42%. Moreover, several studies concluded that the use of the Two-axis instead of the fixed-tilt option significantly increases the generated electricity (Mohammadi et al., 2018; Rad et al. 2020). Therefore, it can be concluded that the value gotten from the present study for each location is compatible with the acceptable values. Consequently, it is technically sustainable to build a grid-connected rooftop PV system in locations. The results indicate that the variation of the EG and CF as a function of location.

Table 4.7: Electricity generation in kWh for the developed systems

Month	Fixed-tilt	Vertical-axis	Two-axis
Jan	463.14	577.68	595.06
Feb	508.70	621.69	632.86
Mar	683.51	865.31	889.23
Apr	710.55	894.45	925.14
May	782.07	1082.26	1140.81
Jun	791.33	1143.50	1207.97
Jul	804.45	1155.24	1218.46
Aug	787.46	1101.50	1156.33
Sep	734.39	956.79	985.10
Oct	663.31	865.31	895.05
Nov	506.09	635.77	654.52
Dec	414.84	518.14	535.48
Annual	7849.83	10417.65	10836.02

4.3.2 Economic sustainability and Emission reduction

The performance of the aforementioned sun-tracking systems is evaluated by the estimation of the economic and environmental factors for each system. In this study, the financial parameters (Table 4.8) inflation rate, discount rate, reinvestment rate, debt ratio, debt interest rate, which are considered as input variables for estimated economic indicators are assumed based on other previous scientific studies. In the present study, the system cost is around $2100-$2600 for 4.65kW PV system, which is estimated based on recent market data in the country and is consistent with cost prices available in the literature.

Table 4.8: Financial parameters

Factor	Unit	Value
Inflation rate	%	2.5
Discount rate	%	3
Reinvestment rate	%	9
Project life	year	25
Debt ratio	%	50
Debt interest rate	%	7
Debt term	year	20
Electricity export escalation rate	%	2

The main results regarding the economic performance of the 4.65kW grid-connected PV system for all developed PV systems are summarized in Table 4.9. The obtained results showed that the value of NPV for the proposed systems is positive and this makes the project to be financially and economically feasible according to Owolabi et al. (2019), Kazem and Khatib (2015) and Rehman et al. (2017). Also, it is found that the proposed projects in the selected locations are economically acceptable based on the internal rate of return, which is a measure of a project’s profitability (Owolabi et al. 2019; Kazem and Khatib 2015; Rehman et al. 2017). .

Moreover, it is observed in Table 4.9, the developed PV project has the longest value of simple payback of 2.68 years for fixed-tilt grid-connected and the lowest one for Two-axis PV system. In addition, it is found that the equity payback values are within the range of 1.26-1.49 years. These results indicate that the PV projects in the selected region make financial sense.

Additionally, it is found that the lowest value of EPC is obtained from Two- axis PV system with a value of 0.0159$/kWh compared to other systems. The EPC value of the proposed projects is compared with the exited value of small-scale PV systems in the literature. It is found that the LCOE values of the proposed systems are within the range of the maximum (3.165$/kWh) and minimum (0.0199$/kWh) of EPC values obtained from the literature. Moreover, it is noticed that the value of EPC is slightly increased by 3% when the fixed-tilt system is used as shown in Table 4.9.

It is noticed that the developed systems are provided a very good insight into the economic viability of the project for all regions. Additionally, the obtained results demonstrated that the development of the proposed 4.65kW PV power system is economically acceptable due to the obtained favorable economic results.

Table 4.9: Economic performance for all developed system

Variable	**Fixed-tilt**	**Vertical-axis**	**Two-axis**
Gross annual GHG emission reduction [tCO_2]	5.75	7.63	7.94
Simple payback [Year]	2.68	2.40	2.31
Equity payback [Year]	1.49	1.32	1.26
Net Present Value (NPV) [USD]	14805.23	19993.24	20916.86
Annual life cycle savings [USD/year]	850.23	1148.17	1201.21
Energy production cost [USD/kWh]	0.0185	0.0166	0.0159

4.3.3 Variation of electrical Production

As mentioned previously, the mean total energy consumption for the chosen household is found to be about 9940kWh. Also, the total annual energy generating from PV systems is varied from 7849.83-10836.02kWh. Figure 10 shows the monthly average electrical energy produced by the proposed PV system of 4.65 kW and the electrical energy purchased from the grid for various PV systems. The results indicate that the PV system of 4.65kW covers almost household and RO desalination plant l load throughout the year as shown in Figure 10. In addition, it is observed that the proposed system covers the total energy consumption for a month of July and August as shown in Figure 4.8.

Furthermore, it is observed that around 40% out of the total energy consumption is covered by the grid and the remaining energy consumption is supplied by PV systems during the winter season. This is due to a heavy electrical load connected in the system like a water heater during winter season. For the other seasons, The PV systems could cover all the energy consumption due to normal environmental parameters such as air temperature, relative humidity, amount of solar radiation, sunshine duration, and so on. Also, due to the length of day that depends on sun altitude, the geographical latitude of the location, declination angle of the sun, and hour angle, the amount of energy production from the PV system will be increased.

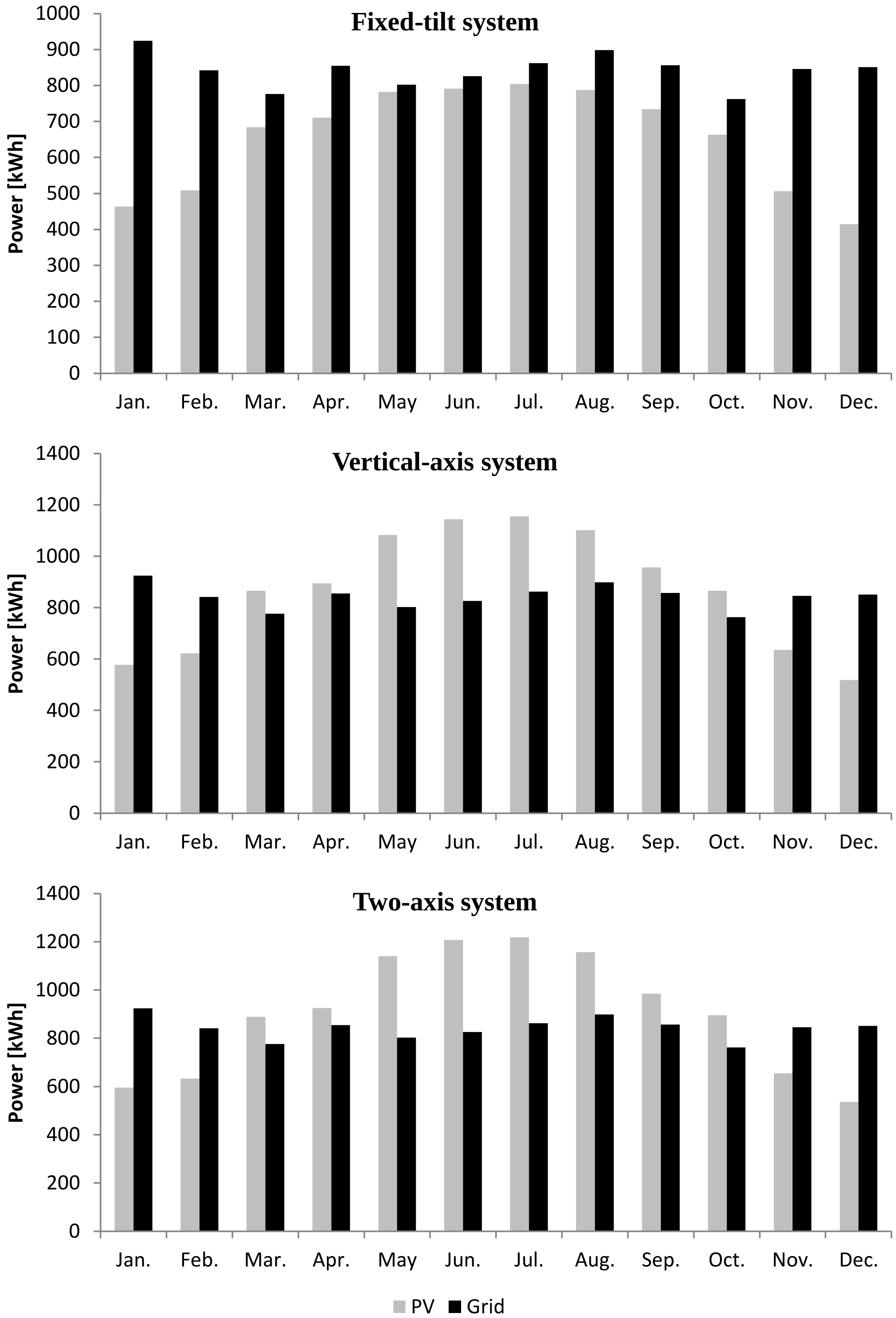

Figure 4.8: Monthly variation of energy generation from PV system and grid

CHAPTER 5
LIMITATIONS AND CONCLUSIONS

5.1 Limitations

Before starting the main conclusions in the present study, it is essential to acknowledge the limitations of this work.

- First, the financial parameters were assumed based on historical values in the literature.
- Second, the influence of various parameters such as dust, irradiation intensity, air temperature, and relative humidity was neglected due to the limitation of RETScreen software.
- Third, the cost of the proposed projects was estimated based on the existing cost in the literature.

5.2 Conclusions

Due to rising electricity tariff rates and reducing the dependency on domestic power generators, installing renewable energy systems has become increasingly attractive for residential consumers, which is supported by previous scientific studies.

Also, due to a lack of detailed study about determining the suitable probability distribution models for analyzing the characteristics of wind speeds in Northern Cyprus, the finding from the present study showed that Burr (4P) and Wakeby are considered as an effective distribution for estimating the wind speed distribution in the selected region. It is found that the value of wind power density is found to be about 11W/m^2, which is classified as poor according to the classification of wind power density at 10m height. Thus, it can be concluded that the high-scale wind turbines are not suitable to generate electricity from wind energy in the selected region.

Furthermore, the analysis indicated that the selected region has a high potential for generating electricity from solar energy compared to wind energy. The results demonstrate that the average annual electrical energy from the Two-axis tracking system was found to be around 10836 kWh. This amount of energy output would contribute significantly to reduce fossil fuel consumption and CO_2 emissions in the country. It is concluded that the small-scale grid-connected PV system will provide the domestic energy and water needs at an energy production cost lower than the electricity price grid-connected consumers pay.

REFERENCES

Agboola, O. P., & Egelioglu, F. (2012). Water scarcity in North Cyprus and solar desalination research: a review. *Desalination and Water Treatment*, 43(1-3), 29–42. doi: 10.1080/19443994.2012.672195

Ahmad, G., & Schmid, J. (2002). Feasibility study of brackish water desalination in the Egyptian deserts and rural regions using PV systems. *Energy Conversion and Management, 43*(18), 2641-2649. doi:10.1016/s0196-8904(01)00189-3

Akhatov, J., Halimov, A., & Juraev, E. (2011). Performance Study of Small Scale Solar PV Powered RO Desalination System. *Proceedings of the ISES Solar World Congress 2011*. doi:10.18086/swc.2011.07.01

Alavi, O., Mohammadi, K., & Mostafaeipour, A. (2016). Evaluating the suitability of wind speed probability distribution models: A case of study of east and southeast parts of Iran. *Energy Conversion and Management*, 119, 101-108.

Alayat, M., Kassem, Y., & Çamur, H. (2018). Assessment of Wind Energy Potential as a Power Generation Source: A Case Study of Eight Selected Locations in Northern Cyprus. *Energies*, 11(10), 2697. doi:10.3390/en11102697

Al-Karaghouli, A., & Kazmerski, L. L. (2013). Energy consumption and water production cost of conventional and renewable-energy-powered desalination processes. *Renewable and Sustainable Energy Reviews, 24*, 343-356. doi:10.1016/j.rser.2012.12.064

Aparicio, J., Candela, L., Alfranca, O., & García-Aróstegui, J. (2017). Economic evaluation of small desalination plants from brackish aquifers. Application to Campo de Cartagena (SE Spain). *Desalination*, *411*, 38-44. doi:10.1016/j.desal.2017.02.004

Arslan, B., & Akün, E. (2019). Management, contamination and quality evaluation of groundwater in North Cyprus. *Agricultural Water Management, 222*, 1-11. doi:10.1016/j.agwat.2019.05.023

Dodd, C. H. (1993). The Political, social and economic development of Northern Cyprus. Huntingdon: Eothen Press.

Elkiran, G., & Ongul, Z. (2009). Implications of excessive water withdrawals to the environment of Northern Cyprus. *Water and Environment Journal*, 23(3), 245-245. doi:10.1111/j.1747-6593.2009.00192.x

Elkiran, G., Aslanova, F., & Hiziroglu, S. (2019). Effluent Water Reuse Possibilities in Northern Cyprus. *Water*, *11*(2), 191. doi:10.3390/w11020191

Elmaadawy, K., Kotb, K. M., Elkadeem, M., Sharshir, S. W., Dán, A., Moawad, A., & Liu, B. (2020). Optimal sizing and techno-enviro-economic feasibility assessment of large-scale reverse osmosis desalination powered with hybrid renewable energy sources. *Energy Conversion and Management, 224,* 113377. doi:10.1016/j.enconman.2020.113377

Ergil, M. (2000). The salination problem of the Guzelyurt aquifer, Cyprus. *Water Research*, 34(4), 1201-1214. doi:10.1016/s0043-1354(99)00253-5

Ezugbe, E. O., & Rathilal, S. (2020). Membrane Technologies in Wastewater Treatment: A Review. *Membranes, 10*(5), 89. doi:10.3390/membranes10050089

Farhat, N. M., Christodoulou, C., Placotas, P., Blankert, B., Sallangos, O., & Vrouwenvelder, J. S. (2020). Cartridge filter selection and replacement: Optimization of produced water quantity, quality, and cost. *Desalination, 473*, 114172. doi:10.1016/j.desal.2019.114172

Fodhil, F., Bessenasse, M., & Cherrar, I. (2019). Feasibility study of grid-connected photovoltaic system for seawater desalination station in Algeria. *Desalination And Water Treatment, 165*, 35-44. doi:10.5004/dwt.2019.24350

Fornarelli, R., Shahnia, F., Anda, M., Bahri, P. A., & Ho, G. (2018). Selecting an economically suitable and sustainable solution for a renewable energy-powered water desalination system: A rural Australian case study. *Desalination*, 435, 128-139. doi:10.1016/j.desal.2017.11.008

Fritzmann, C., Löwenberg, J., Wintgens, T., & Melin, T. (2007). State-of-the-art of reverse osmosis desalination. *Desalination, 216*(1-3), 1-76. doi:10.1016/j.desal.2006.12.009

Gass, I., & Masson-Smith, D. (1963). The geology and gravity anomalies of the Troodos Massif, Cyprus. Proceedings of the Royal Society of London. *Series B. Biological Sciences*, 157(969), 587-588.

Giannakis, E., Serghides, D., Dimitriou, S., & Zittis, G. (2020). Land transport CO2 emissions and climate change: Evidence from Cyprus. *International Journal of Sustainable Energy, 39*(7), 634-647. doi:10.1080/14786451.2020.1743704

Gökçek, M. (2018). Integration of hybrid power (wind-photovoltaic-diesel-battery) and seawater reverse osmosis systems for small-scale desalination applications. *Desalination, 435,* 210-220. doi:10.1016/j.desal.2017.07.006

Gökçek, M., & Gökçek, Ö B. (2016). Technical and economic evaluation of freshwater production from a wind-powered small-scale seawater reverse osmosis system (WP-SWRO). *Desalination, 381*, 47-57. doi:10.1016/j.desal.2015.12.004

Gökçekuş, H. & Doyuran, V. (1995). Evaluation of hydrochemical data from Güzelyurt Aquifer (Turkish Republic of Northern Cyprus) through Cluster Analysis. *Turkish Journal of Earth Sciences*, 4(1), 1-10

Gökçekuş, H. & Olgun, E. (1993). Cenozoic stratigraphy of the Güzelyurt Basin, Turkish Republic of Northern Cyprus. *TAPG Bulletin*, 5(1), 57–68.

Gökçekuş, H. (1990). Hydrologeological and hydrogeochmiecal evaluation of the Güzelyurt groundwater basin T.R.N.C. Ph. D. Thesis. M.E.T.U. Ankara. p 197.

Gökçekus, H. and Doyuran, V. (1995). Evaluation of Hydrodynamic Data from Güzelyurt Aquifer (Turkish Republic of Northern Cyprus) Through Cluster Analysis. *Tr. J.of Earth Sciences*. 4, 1-10.

Gökçekuş, H.& Doyuran, V. (1998). Groundwater budget for the Güzelyurt Aquifer: An example for an overdraft. Proceedings of the International Conference on Water Problems in the Mediterranean Countries. Lefkoşa, TRNC:NEU, 5(2), 779 – 787.

Gökçekus, H., & Kassem, Y. (2020). Turkey-North Cyprus-Neighboring Countries Peace Water Project. In Cyprus: Alternative Solution Models. Peter Lang Gmbh, Internationaler Verlag Der Wissenschaften.

Gökçekuş, H., & Nourani, V. (2018). Lessons From Groundwater Quantity and Quality Problems In the Güzelyurt Coastal Aquifer, North Cyprus. In Advances in Environmental Research (Vol. 64). Nova Science Publishers, Inc.

Gökçekuş, H., Doyuran, V. (1997a). Evaluation of domestic and agricultural quality of the groundwater in the Güzelyurt Basin (North Cyprus). Proceedings of the

International Conference on Water Problems in the Mediterranean Countries 11, 1305–1314.

Gökçekuş, H., Doyuran, V. (1997b). Groundwater budget for the Güzelyurt basin (North Cyprus). Proceedings of the International Conference on Water Problems in the Mediterranean Countries 11, 779–787.

Gökçekuş, H., Türker, U., Sözen, S., & Orhon, D. (2002). Water management difficulties with limited and contaminated water resources. *International conference on the Environmental Problem of the Mediterranean region* (pp. 1241-1249).

Gold, G., & Webber, M. (2015). The Energy-Water Nexus: An Analysis and Comparison of Various Configurations Integrating Desalination with Renewable Power. *Resources*, 4(2), 227-276. doi:10.3390/resources4020227

Greenlee, L. F., Lawler, D. F., Freeman, B. D., Marrot, B., & Moulin, P. (2009). Reverse osmosis desalination: Water sources, technology, and todays challenges. *Water Research, 43*(9), 2317-2348. doi:10.1016/j.watres.2009.03.010

Hoslett, J., Massara, T. M., Malamis, S., Ahmad, D., Boogaert, I. V., Katsou, E., . . . Jouhara, H. (2018). Surface water filtration using granular media and membranes: A review. *Science of The Total Environment, 639,* 1268-1282. doi:10.1016/j.scitotenv.2018.05.247

Kahramanoğlu, I., Usanmaz, S., & Alas, T. (2020). Water footprint and irrigation use efficiency of important crops in Northern Cyprus from an environmental, economic and dietary perspective. *Saudi Journal of Biological Sciences, 27*(1), 134-141. doi:10.1016/j.sjbs.2019.06.005

Kassem, Y. Gökçekuş, H. & Çamur, H. (2018). Economic assessment of renewable power generation based on wind speed and solar radiation in urban regions. *Global J. Environ. Sci. Manage.*, 4(4),465-482.

Kassem, Y., Al Zoubi, R., & Gökçekuş, H. (2019). The possibility of generating electricity using small-scale wind turbines and solar photovoltaic systems for households in Northern Cyprus: a comparative study. *Environments*, 6(4), 47.

Kassem, Y., Çamur, H., & Alhuoti, S. M. (2020). Solar Energy Technology for Northern Cyprus: Assessment, Statistical Analysis, and Feasibility Study. *Energies,* 13(4), 940. doi:10.3390/en13040940

Kassem, Y., Çamur, H., & Alhuoti, S. M. A. (2020). Solar Energy Technology for Northern Cyprus: Assessment, Statistical Analysis, and Feasibility Study. *Energies,* 13(4), 940.

Kassem, Y., Gökçekuş, H, Çamur, H., & Esenel, E. (2020). Statistical analysis and determination of best-fit probability distribution for monthly rainfall in Northern Cyprus. *Desalination and Water Treatment*. doi: 10.5004/dwt.2020.26556

Kassem, Y., Gökçekuş, H., & Zeitoun, M. (2019). Modeling of techno-economic assessment on wind energy potential at three selected coastal regions in Lebanon. *Modeling Earth Systems and Environment,* 5(3), 1037-1049. doi:10.1007/s40808-019-00589-9

Khan, M. A., Çamur, H., & Kassem, Y. (2019). Modeling predictive assessment of wind energy potential as a power generation sources at some selected locations in Pakistan. *Modeling Earth Systems and Environment*, 5(2), 555-569.

Khan, M. A., Rehman, S., & Al-Sulaiman, F. A. (2018). A hybrid renewable energy system as a potential energy source for water desalination using reverse osmosis: A review. *Renewable and Sustainable Energy Reviews, 97*, 456-477. doi:10.1016/j.rser.2018.08.049

Khandelwal, A., & Shrivastava, V. (2017). Viability of grid-connected solar PV system for a village of Rajasthan. In 2017 International Conference on Information, Communication, Instrumentation and Control (ICICIC) (1-6). IEEE.

Khiari, W., Turki, M., & Belhadj, J. (2019). Power control strategy for PV/Wind reverse osmosis desalination without battery. *Control Engineering Practice, 89*, 169-179. doi:10.1016/j.conengprac.2019.05.020

Kim, J., Park, K., Yang, D. R., & Hong, S. (2019). A comprehensive review of energy consumption of seawater reverse osmosis desalination plants. *Applied Energy, 254*, 113652. doi:10.1016/j.apenergy.2019.113652

Ko, W., Lee, J., & Ham, C. (2013). A Grid-Connected Desalination Plant Operation. Systemics, *Cybernetics and Informatics,* 11(1), 79-83.

Lau, K. K. L., Lindberg, F., Johansson, E., Rasmussen, M. I., & Thorsson, S. (2017). Investigating solar energy potential in tropical urban environment: A case study of Dar es Salaam, Tanzania. *Sustainable cities and Society,* 30, 118-127.

Li, Q., Lian, B., Wang, Y., Taylor, R. A., Dong, M., Lloyd, T., . . . Leslie, G. (2018). Development of a mobile groundwater desalination system for communities in rural India. *Water Research, 144*, 642-655. doi:10.1016/j.watres.2018.08.001

Maammeur, H., Hamidat, A., Loukarfi, L., Missoum, M., Abdeladim, K., & Nacer, T. (2017). Performance investigation of grid-connected PV systems for family farms: case study of North-West of Algeria. *Renewable and Sustainable Energy Reviews,* 78, 1208-1220.

Mahmoudi, H., Spahis, N., Goosen, M. F., Sablani, S., Abdul-Wahab, S. A., Ghaffour, N., & Drouiche, N. (2009). Assessment of wind energy to power solar brackish water greenhouse desalination units: A case study from Algeria. *Renewable and Sustainable Energy Reviews, 13*(8), 2149-2155. doi:10.1016/j.rser.2009.03.001

Mansouri, A. E., Hasnaoui, M., Amahmid, A., & Hasnaoui, S. (2020). Feasibility analysis of reverse osmosis desalination driven by a solar pond in Mediterranean and semi-arid climates. *Energy Conversion and Management, 221*, 113190. doi:10.1016/j.enconman.2020.113190

Mason, M. (2020). Hydraulic patronage: A political ecology of the Turkey-Northern Cyprus water pipeline. *Political Geography, 76,* 102086. doi:10.1016/j.polgeo.2019.102086

Masseran, N. (2015). Evaluating wind power density models and their statistical properties. Energy, 84, 533-541.

Mehmood, A., Shaikh, F. A., & Waqas, A. (2014). Modeling of the solar photovoltaic systems to fulfill the energy demand of the domestic sector of Pakistan using RETSCREEN software. In 2014 International Conference and Utility Exhibition on Green Energy for Sustainable Development (ICUE) (pp. 1-7). IEEE.

Monjezi, A. A., Chen, Y., Vepa, R., Kashyout, A. E., Hassan, G., Fath, H. E., . . . Shaheed, M. H. (2020). Development of an off-grid solar energy powered reverse osmosis desalination system for continuous production of freshwater with integrated photovoltaic thermal (PVT) cooling. *Desalination, 495*, 114679. doi:10.1016/j.desal.2020.114679

Moser, M., Trieb, F., Fichter, T., & Kern, J. (2013). Renewable desalination: A methodology for cost comparison. *Desalination and Water Treatment*, 51(4-6), 1171-1189. doi:10.1080/19443994.2012.715446

Mostafaeipour, A., Qolipour, M., Rezaei, M., & Babaee-Tirkolaee, E. (2019). Investigation of off-grid photovoltaic systems for a reverse osmosis desalination system: A case study. *Desalination, 454*, 91-103. doi:10.1016/j.desal.2018.03.007

Muñoz, I., & Fernández-Alba, A. R. (2008). Reducing the environmental impacts of reverse osmosis desalination by using brackish groundwater resources. *Water Research*, *42*(3), 801-811. doi:10.1016/j.watres.2007.08.021

Nacer, T., Hamidat, A., Nadjemi, O., & Bey, M. (2016). Feasibility study of grid connected photovoltaic system in family farms for electricity generation in rural areas. *Renewable Energy*, 96, 305-318.

Ouarda, T. B., Charron, C., Shin, J. Y., Marpu, P. R., Al-Mandoos, A. H., Al-Tamimi, M. H., ... & Al Hosary, T. N. (2015). Probability distributions of wind speed in the UAE. *Energy conversion and management*, 93, 414-434.

Papadopoulou, M., Charchousi, D., Spanoudaki, K., Karali, A., Varotsos, K., Giannakopoulos, C., . . . Loizidou, M. (2020). Agricultural Water Vulnerability under Climate Change in Cyprus. *Atmosphere, 11*(6), 648. doi:10.3390/atmos11060648

Park, E. J. (2020). Strategy of Water Distribution for Sustainable Community: Who Owns Water in Divided Cyprus? *Sustainability, 12*(21), 8978. doi:10.3390/su12218978

Payab, A. H., & Türker, U. (2019). Comparison of standardized meteorological indices for drought monitoring at northern part of Cyprus. *Environmental Earth Sciences, 78*(10). doi:10.1007/s12665-019-8309-x

Payab, A. H., Banihabib, M. E., & Türker, U. (2020). Scrutinizing the simultaneous impact of drought on irrigated agriculture and groundwater resources. *Desalination And Water Treatment, 177*, 363-373. doi:10.5004/dwt.2020.24915

Peng, W., Maleki, A., Rosen, M. A., & Azarikhah, P. (2018). Optimization of a hybrid system for solar-wind-based water desalination by reverse osmosis: Comparison of approaches. *Desalination, 442*, 16-31. doi:10.1016/j.desal.2018.03.021

Prăvălie, R., Patriche, C., & Bandoc, G. (2019). Spatial assessment of solar energy potential at global scale. A geographical approach. *Journal of Cleaner Production*, 209, 692-721.

Searle, D.L., & Panayiotou, A. (1980) structural implications in the evaluation of the Troodos massif, Cyprus. In ophiolites , international Ophiolite Symposium, edited by A. Panayitou, Proceedings, 50-60.

Semiat, R. (2008). Energy Issues in Desalination Processes. *Environmental Science & Technology*, 42(22), 8193-8201. doi:10.1021/es801330u

Siddiqi, A., & Anadon, L. D. (2011). The water–energy nexus in Middle East and North Africa. *Energy Policy,* 39(8), 4529-4540. doi:10.1016/j.enpol.2011.04.023

Sofroniou, A., & Bishop, S. (2014). Water Scarcity in Cyprus: A Review and Call for Integrated Policy. Water, 6(10), 2898-2928. doi:10.3390/w6102898

Triki, Z., Bouaziz, M., & Boumaza, M. (2013). Techno-economic feasibility of wind-powered reverse osmosis brackish water desalination systems in southern Algeria. *Desalination and Water Treatment*, *52*(7-9), 1745-1760. doi:10.1080/19443994.2013.807040

Türker, U., & Hansen, B. R. (2012).River Basin Management and Characterization of Water Bodies in North Cyprus. 10th International Congress on Advances in Civil Engineering,7-19 October 2012 Middle East Technical University, Ankara, Turkey.

Türkman, F. & Elkıran, G. (2008). Water Resources and Planning in TRNC- Kuzey Kıbrıs Türk Cumhuriyeti‟nde Su Kaynakları ve Planlaması" TMMOB İMO 2. Congress on Water Policies Proceedings, Pg.425 İMO, Ankara

Vakili-Nezhaad, G., Mishra, S. B., Mousa, H., & Ziaiefar, H. (2020). Simulation and optimization of hybrid green energy systems for desalination purposes. *Environmental Progress & Sustainable Energy*. doi:10.1002/ep.13515

World Water Assessment Programme. (2015). The UN World Water Development Report 2015, Water for a Sustainable World. Retrieved January 1, 2021, from http://www.unesco.org/new/en/natural-sciences/environment/water/wwap/wwdr/2015-water-for-a-sustainable-world/

Wright, N. C., & Winter, A. G. (2014). Justification for community-scale photovoltaic-powered electrodialysis desalination systems for inland rural villages in India. *Desalination, 352*, 82-91. doi:10.1016/j.desal.2014.07.035

Wu, B., Maleki, A., Pourfayaz, F., & Rosen, M. A. (2018). Optimal design of stand-alone reverse osmosis desalination driven by a photovoltaic and diesel generator hybrid system. *Solar Energy*, *163*, 91-103. doi:10.1016/j.solener.2018.01.016

Yıldırım, S., Asilsoy, B., & Özden, Ö. (2020). Urban Resident Views About Open Green Spaces: A Study in Güzelyurt (Morphou), Cyprus. *European Journal of Sustainable Development*, *9*(2), 441-450. doi:10.14207/ejsd.2020.v9n2p441

Yildiz, D., & Çakmak, C. (2014). Peace River to Cyprus from Turkey (pp. 1-34, Publication). Ankara: Hydropolitics Academy.

APPENDICES

APPENDIX 1

ETHICAL APPROVAL LETTER

YAKIN DOĞU ÜNİVERSİTESİ

ETHICAL APROVAL DOCUMENT

Date: 21/06 /2021

To the **Graduate School of Applied Sciences**

The research project titled ‘’ Modeling Predictive Suitability to Estimate the Potential of Wind and Solar Energy to Power Water Desalination Units in Güzelyurt Region, Northern Cyprus’’ has been evaluated. Since the researcher(s) will not collect primary data from humans, animals, plants or earth, this project does not need through the ethics committee.

Title: Assist. Prof. Dr.

Name Surname: Anoosheh Iravanian

Signature:

Role in the Research Project: Supervisor

Title: Assoc. Prof. Dr.

Name Surname: Youssef Kassem

Signature:

Role in the Research Project: Co-Supervisor

APPENDIX 2

SIMILARITY REPORT

turnitin

Assignments | Students | Grade Book | Libraries | Calendar | Discussion | Preferences

NOW VIEWING: HOME > PAPER > RIFAT GÖKÇEKUŞ, MODELING PREDICTIVE SUITABILITY TO ESTIMATE THE POTENTIAL OF WIND AND SOLAR ENERGY TO POWER WATER DESALINATION UNITS IN GÜZELYURT REGION, NORTHERN CYPRUS

About this page

This is your assignment inbox. To view a paper, select the paper's title. To view a Similarity Report, select the paper's Similarity Report icon in the similarity column. A ghosted icon indicates that the Similarity Report has not yet been generated.

RIFAT GÖKÇEKUŞ, MODELING PREDICTIVE SUITABILITY TO...

INBOX | NOW VIEWING: NEW PAPERS ▾

Submit File

Online Grading Report | Edit assignment settings | Email non-submitters

AUTHOR	TITLE	SIMILARITY	GRADE	RESPONSE	FILE	PAPER ID	DATE
Rifat Gökçekuş	Abstract	0%	--	--		1610073046	21-Jun-2021
Rifat Gökçekuş	chapter 4	0%	--	--		1610077341	21-Jun-2021
Rifat Gökçekuş	chapter 5	0%	--	--		1610078147	21-Jun-2021
Rifat Gökçekuş	chapter 1	5%	--	--		1610073317	21-Jun-2021
Rifat Gökçekuş	chapter 2	8%	--	--		1610073880	21-Jun-2021
Rifat Gökçekuş	chapter 3	10%	--	--		1610076755	21-Jun-2021
Rifat Gökçekuş	All Thesis	12%	--	--		1610079187	21-Jun-2021